NAVAL POSTGRADUATE SCHOOL

THE DEFLECTION OF PLANE TURBULENT JETS BY CONVEX WALLS

by

TURGUT SARPKAYA
Department of Mechanical Engineering

27 June 1968

NAVAL POSTGRADUATE SCHOOL
Monterey, California

Rear Admiral R. W. McNitt, USN
Superintendent

R. F. Rinehart
Academic Dean

ABSTRACT:

The effects of geometry and Reynolds number on the attachment of a jet to a convex wall and the mechanism of high pressure recovery in convex-walled amplifiers are investigated. The results are presented in terms of normalized parameters in a form suitable for comparison with theoretical results. Reasonably good agreement is obtained between the experimental results and those predicted theoretically by Gortler and Glauert, particularly for regions of flow away from the control port. The effects of the wall setback and control port are most pronounced in a region near the power nozzle where u_m/U_o attains values as high as 1.25.

This task was supported by: Harry Diamond Laboratories
U. S. Army Materiel Command
Contract No. MIPR #R-68-4

C. E. Menneken
Dean of Research Administration

NPS-59SL8061A

27 June 1968

FOREWORD

The research described in this report is a part of work initiated under the general research program of the Harry Diamond Laboratories of the U. S. Army Materiel Command on the characteristics of load-insensitive, convex-walled, bistable amplifiers. A comprehensive experimental study of the performance characteristics of bistable amplifiers with straight, convex, and concave-walled amplifiers was reported in the previous annual report "NU Hydro-Report No. 033-TS, July 1967" and in the paper entitled "The Comparative Performance Characteristics of Vented and Unvented, Cusped, and Straight and Curved-Walled Bistable Amplifiers" by T. Sarpkaya and Joseph M. Kirshner, Paper F3, Third Cranfield Fluidics Conference, 8-10 May, 1968, Turin.

TABLE OF CONTENTS

TABLE OF SYMBOLS

b	Power jet width
J	Jet momentum per unit span of slot = $\rho U_o^2 b$
p_w	Static pressure on the surface of the cylinder
P_s	Stagnation pressure of the fluid supplying the jet
R	Radius of the quadrant
Re_w	Reynolds number = $U_o b/\nu$
u	Local fluid velocity
u_m	Maximum velocity in a given profile
U_o	Average velocity of the power jet
y	Radial distance from the wall
y_m	Radial distance from the wall to the maximum velocity
$y_{m/2}$	Radial distance from the wall to the point where the local velocity is one half of the maximum velocity
θ	Angular position
ν	Kinematic viscosity of fluid
ρ	Density of fluid
σ	A constant

TABLE OF FIGURES

INTRODUCTION

The most critical parameters affecting the performance of a bistable amplifier are the sidewall setback, splitter location, receiving aperture width, location of vents, splitter-cusp radius, and the shape of the Coanda-walls. The effect of the variation of all these parameters has previously been investigated and reported by Sarpkaya (1) and Sarpkaya and Kirshner (2). It has been concluded that a vented, convex-walled amplifier exhibits nearly ideal performance characteristics and that the understanding of the underlying reasons could only come from an extensive study of the attachment and separation of a turbulent jet to and from a curved surface set back relative to the power jet and control port.

Most of the researchers in the field of fluidics dealt with straight-walled amplifiers. The attachment of a fluid jet to a curved wall and its subsequent separation has been used by some investigators as the basis of a fluid amplifier element. Researchers in the U.S.S.R. used an air foil geometry and supply jet exiting tangentially to the surface (3). A control jet opposed to the supply jet induced early separation. Curtiss, Liquornic, and Feil employed separation from a curved surface in a curved elbow amplifier (4, 5). Kadosch (6) studied the separation of jets from curved surfaces and used the principle in a fluidic oscillator. In all of these devices, the separation of the jet from the curved surface is controlled by a small secondary flow injected into a boundary layer. The performance of these devices depends on the proper selection of the geometry and the parameters associated with it.

Newman (7) and Kadosch (6) studied the separation of a jet with turbulent boundary layer from a curved wall. In these studies, one lip of a two-dimensional slot was assumed to extend in the form of a circular cylinder and there was, in the geometry chosen, neither a control port nor a setback. McGlaughlin and Greber (8) carried out experiments on such a curved-wall device for Reynolds numbers below the critical range and investigated the feasibility of the development of an electro-pneumatic converter by heating the curved wall. Although most of these studies were conducted for the purpose of developing suitable fluidic devices, part of the attention was due to the possibility of obtaining thrust-vector control for applications on V/STOL aircraft. The possibility of thrust augmentation due to air entrainment and increased mass flow in the jet sheet has been considered by Bailey (9), Von Glahn (10), Mehus (11), Von Karman (12), and McKinney (13). Some of the lifting devices employed on V/STOL vehicles such as the jet-augmented flap exhibit behavior similar to that of the Coanda flow about curved surfaces.

It is apparent from the foregoing discussion that the information derived from a comprehensive study of the flow over a curved surface would have broad applications not only to all fluidic devices derivable from flow over curved surfaces but also to other related fields such as the development of V/STOL aircraft.

The hydrodynamic analysis of the turning of laminar or turbulent plane jet sheets is rather incomplete. At low Reynolds numbers, the laminar jet separates from the curved surface after only a relatively short distance from the jet exit. The separated jet becomes turbulent some distance downstream of the separation point. At some critical Reynolds

number, the turbulent jet reattaches to the surface. This results in an enclosed separation bubble. The reattached turbulent jet again separates at a point downstream of the bubble. As the Reynolds number is further increased, the reattachment point moves upstream, but the separation points do not change significantly. The bubble size decreases with increasing Reynolds numbers and finally vanishes. According to the measurements of Liepman and Laufer (14), transition in a free jet occurs at a distance 7×10^4 ν/U from the exit. The mixing layers finally emerge in the center of the jet and if Ub/ν is sufficiently large, a fully turbulent jet is obtained about 10b downstream of the exit. Newman (7), in the case of a two-dimensional jet round a circular cylinder, found that the transition in the outer part of the emerging flow occurs at a distance of about 3×10^4 ν/U and in the inner boundary layer in a region extending from 2×10^4 ν/U to 7×10^4 ν/U.

By considering the flow in the hodograph plane, potential theories have been obtained by Lighthill (15), Metral (16), Metral and Zerner (17), and Yen (18) for two-dimensional incompressible jets flowing round various cylindrical shapes with the surrounding fluid at rest. These theories predicted an increased mass flow from the slot but of necessity neglected the entrainment of the surrounding fluid by the jet and failed to predict either the reattachment of the jet flow to the surface or its final separation from the surface.

Two additional theoretical studies which have some bearing on the present study are due to Görtler (19) and Glauert (20). Görtler, assuming the eddy viscosity to be constant across the flow at each x and therefore

proportional to $u_m y_{m/2}$, obtained a solution for the local mean velocity in a two-dimensional free turbulent jet as

$$u = u_m \operatorname{sech}^2 \frac{0.88\, y}{y_{m/2}} \tag{1}$$

or

$$= \left[\frac{3\,\sigma}{4\,\rho\,x}\right]^{1/2} \operatorname{sech}^2 \frac{\sigma y}{x}$$

where σ is a constant. The measurements of Reichardt (21) and Förthmann (22) indicated that for small values of x/b, the flow was not independent of the nozzle width b, and that σ varied from 12 near the nozzle to 7.7 at large values of x/b.

Glauert (19), who introduced the term "wall jet", obtained solutions for both laminar and turbulent, radial and plane wall jets. The mean velocity profile consisted of an inner boundary layer ($y < y_m$) and an outer half jet. The inner profile for the plane turbulent wall jet, as computed numerically by Glauert, is shown in Fig. 1. The [illegible] file is similar to that of a free jet and is given by

$$\frac{u}{u_m} = \operatorname{sech}^2 \left[0.88 \frac{y - y_m}{y_{m/2} - y_m}\right] \tag{2}$$

Measurements in a plane turbulent wall jet have been carried out by Förthmann (22) and Sigalla (23) for values of $u_m(y_{m/2} - y_m)/\nu$ ranging from

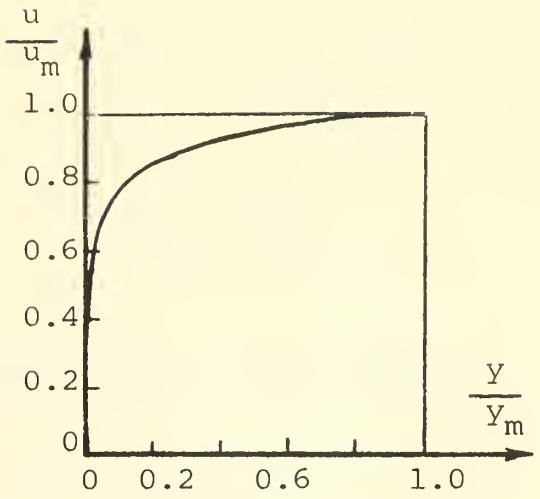

Fig. 1 Boundary Layer Mean Velocity Profile of the Turbulent Wall Jet

3.5×10^4 to 9×10^4, and it was found that $y_m/y_{m/2}$ remains nearly constant at about 0.15. The experiments have also shown that the eddy viscosity in the outer part of the wall jet is smaller than that of a free jet. This conclusion, as will be seen later, is dependent upon the shape of the bounding wall.

Newman (7) carried out a dimensional analysis for the flow of a two-dimensional, incompressible, turbulent jet round a circular cylinder where one lip of the nozzle of width b joins the cylinder tangentially (no setback or control port), and found that, for large values of the Reynolds number,

$$\frac{p_w}{p_s}\,\frac{R}{b} = f(\theta) \quad \text{and} \quad \theta_{sep} = f\left[\frac{b}{R}\,,\ \frac{p_s R\, b}{\rho \nu^2}\right] \qquad (3)$$

For angular positions sufficiently far from the nozzle, θ_{sep} ceases to be a function of b/R, and for sufficiently large Reynolds numbers it remains nearly constant. Furthermore, measurements of Newman have shown that $y_{m/2}$, R and θ may be correlated empirically by

$$\frac{y_{m/2}}{R\,\theta} = 0.11 \left(1 + 1.5 \frac{y_{m/2}}{R} \right) \qquad (4)$$

which represents a straight line in terms of $y_{m/2}/R\,\theta$ versus $y_{m/2}/R$. A comparison of the results obtained from Eq. (4) with those obtained for a plane wall jet shows that the flow round a circular cylinder spreads more rapidly than a wall jet and that for $y/y_{m/2} > 0.05$, the effective eddy viscosity is similar to that of a free jet. Newman attributed the latter to an increased mixing associated with the flow curvature in the outer part of the flow.

The ultimate objective of the investigation reported herein is the understanding of the complex mechanism which provides a convex-walled vented amplifier with pressure recoveries which are in excess of those obtained by an analysis based on isentropic flow assumption. To this end, the first part of the study has been devoted to the understanding of the characteristics of flow over convex walls (without vents) and to the accumulation of velocity and pressure data. The method of securing data and the comparison of the experimental and theoretical results are subsequently presented.

EXPERIMENTAL EQUIPMENT AND PROCEDURE

The arrangement of the experimental apparatus is shown in Fig. 2. Air, at approximately 170 psig, was supplied to the system through a series of pressure regulators and an appropriately sized, calibrated rotameter. Pressures at the rotameter, power jet, and at the pressure taps along the convex wall were monitored by a differential-pressure transducer. Individual pressure readings were taken by opening and closing appropriate valves on a common pressure manifold. The output of the pressure transducer was monitored by a two-channel amplifier-recorder system.

A Pitot tube coupled with a micrometer barrel was used to take the velocity profiles. Velocities were measured at various angular positions along the radial lines in the mid-plane of the quadrant.

Test Section

The test section was fabricated from a sheet of one-inch plexiglas placed between two 1/2" sheets of plexiglas (see Figs. 3 and 4). The two movable sections which bound the power jet were cut to appropriate dimensions and then cut to final dimensions on a milling machine. The static pressure tap for the power jet was then drilled in the upper panel and the faces in contact with the fluid were given a final hand polishing with rouge. The upper and lower panels were then clamped with a 1/4" gage block between them for the power jet. The two panels were then glued together at the entrance end with a "T" block which provided the transition from the inlet tube to the rectangular power jet.

A circular block was cut out of a one-inch plate to form the quadrant. After machining the block to approximately a ten-inch diameter, the pressure taps were drilled in the periphery. These holes were drilled with a #67 drill, on an indexing head, every 6 degrees; staggered 1/16" off center as follows: center line, 1/16" left of center line, 1/16" right of center line, center line, etc. The quadrant was then cut out of the block and all surfaces were carefully polished.

In order to make the panel assembly movable in two directions and thus to provide for variable setbacks and control port widths, 1/4" square holes were provided around all edges of the panel assembly at approximately two-inch intervals. The panel assembly was made movable instead of the quadrant because of the large number of pressure taps emanating from the quadrant.

The two side plates were made of 1/2" plexiglas sheets. A circular slot for the Pitot tube jig was machined in both side plates. These slots had a common center of curvature with the quadrant to ensure consistent radial settings of the Pitot tube. The quadrant was then dowelled to one of the side plates as a reference. The panel assembly was then placed next to the quadrant to establish the zero setback condition with a depth micrometer. The test section was completed by placing the other side plate on top of the quadrant and the panel assembly, and bolting the resulting assembly together.

Procedure

Each run consisted of first selecting a proper setback, flow rate, and control port condition (open or closed). Then the following

parameters were recorded: (1) atmospheric pressure and temperature; (2) rotameter outlet pressure; (3) power jet wall pressure; (4) wall pressures along the quadrant (14 taps); and (5) velocity readings every 0.05" from the quadrant and every 12° along the quadrant.

Each one of the three setbacks used (0.025", 0.050", and 0.075") was set into the test section with a depth micrometer. A 1/4" gage block was inserted into the control port during the above measurement to maintain the parallelism of the sides of the control port. This was necessary because the control port boundaries were formed by the quadrant and panel assembly which are not directly coupled.

The flow rate was established with the use of a calibrated rotameter and six flow rates were used for each setback and control port condition. These flow rates resulted in Reynolds numbers (based on the hydraulic diameter of the power jet) ranging from approximately 16,000 to 35,000. Or, in terms of the Reynolds number based on the power jet width of 1/4", from approximately 9,800 to 22,000.

The calibration of the system was accomplished by connecting a pressure transducer and a micromanometer to a pressure manifold. The atmospheric reference valve was opened and the manometer zeroed. Then the reference valve was closed and the valve from the power jet pressure tap was opened to provide a pressure source. The flow rate was then adjusted until the manometer again was zeroed on 1" of water. By adjusting the gain of the amplifier, a full scale deflection of 50 mm was achieved with attenuation on position #1. The linearity of the recording system was checked with various amounts of pressure. No deviation from the straight calibration curve was detected.

After selecting the setback and choosing the condition of the control port, and balancing and calibrating the recorder, a typical run was made as follows:

(1) A specific flow rate was set with the rotameter;

(2) The reference valve was opened and the recorder positioned to zero;

(3) The reference valve was closed and the rotameter outlet pressure valve was opened;

(4) After the pressure was recorded, the pressure valve was closed and the reference valve was again opened, thus referencing the pressure readings to atmospheric pressure;

(5) The above procedure was repeated for the power jet pressure and the 14 pressure taps along the quadrant;

(6) With the valve manipulation remaining the same, the velocity profiles were taken at 6, 18, 30, 42, 54, 66, and 78 degrees around the quadrant.

The data obtained through the procedure described above have been normalized through the use of appropriate parameters and are presented graphically in the next section.

DISCUSSION OF RESULTS AND CONCLUSIONS

Firstly, various pressure and velocity profiles and the overall characteristics of flow will be discussed. Finally, a comparison will be made between the experimental results and those obtained from the analyses of Görtler and Glauert.

Figures 5 and 6 present the normalized pressure p_w/P_s versus the angle θ for the setbacks of 0.025" and 0.075", for a Reynolds number of 12,300, and for both open and closed control-port conditions. It is apparent from these two plots that there is a large number of pressure oscillations near the nozzle and particularly for smaller setbacks. The nonuniformity of the pressure distribution along the wall and the instability of the jet are in essence commonly observed flow characteristics in fluid amplifiers with relatively small setbacks. The mechanism which causes the pressure oscillations is not well understood. Similar oscillations are also observable on the data presented by Newman for the case of a tangential jet flow round a circular cylinder. Newman preferred to represent his data with a mean curve and made no mention of the pressure oscillations.

Extensive and repeated measurements of the wall pressures along the quadrant have verified the existence of pressure oscillations with resulting modifications of the velocity distribution in the boundary layer. It is quite possible that for very small setbacks, the jet is undergoing a series of attachments, separations, and reattachments within a region close to the nozzle or the control port. As the setback increases, the low pressure region remains fairly constant and extends as far as 60

degrees from the outlet of the power jet and shortly thereafter the wall pressure rises sharply. Although it is not possible to assign a specific angular position to the point of separation, Figs. 5 and 6 show that the separation point (A better terminology would be "separation zone".) is approximately between $\theta = 85°$ and 90°. It is further observed that as the setback increases, the magnitude of the normalized pressure P_w/P_s remains relatively constant until separation occurs. This is true even though the magnitude of the wall pressure does not change significantly. It is obvious that the increased setback leads to a more stable reattachment. It should also be noted that the separation point is relatively insensitive to the amount of setback even though the point of separation is not as clearly defined for smaller setbacks as it is with larger setbacks.

Figures 7-12 show the normalized velocity profiles for a Reynolds number of 12,300 for the two setbacks of 0.025" and 0.075" and for various angular positions and control port conditions. It is immediately apparent from the data that the effect of the control port condition on the velocity profile is most significant on the profiles closer to the power jet than on those at larger angles. As a matter of fact, it is for this very reason that the experimental velocity distributions for the region under consideration deviate more significantly from those predicted theoretically as will be discussed later. It should, however, also be noted that a good agreement is not expected in view of the fact that the assumptions governing the theories due to Görtler and Glauert do not include, among other things, either the presence of a control port or of a setback.

It is also apparent from Figs. 7-12 that the closed control port condition produces a velocity profile whose maximum occurs relatively closer to the curved wall. In other words, the jet, as would be anticipated, is "pulled" closer to the boundary due to the vacuum established in the control port. The difference in the velocity profiles due to various control port conditions diminishes rapidly as the angular position increases, i.e., as the jet gets farther away from the nozzle. The difference in the velocity profiles due to various control port conditions diminishes rapidly as the distance to the section under consideration increases.

Figures 13 and 14 show the normalized pressure distributions, similar to those presented in Figs. 5 and 6, for a Reynolds number of 20,200. The observations regarding the condition of the control port remain valid for this particular Reynolds number also. Once again the magnitude of the normalized pressure p_w/P_s remains essentially unchanged for the two values of setback. Furthermore, not only is the parameter p_w/P_s relatively insensitive to setback but also to Reynolds number.

Figures 15 through 20 present the velocity profiles as before except for Re = 20,200. The data bear out once again the effect of the vacuum provided by the closed control port on the position of the jet, and on the velocity distribution.

Figures 21 through 26 present a comparison of the normalized velocity profiles for Re = 20,200 with those obtained from the analyses of Görtler and Glauert. The comparison is presented only for the open control port condition. As anticipated, the effect of the control port and the setback

on the velocity profile, which are not present in the theoretical analysis, is most evident for the angular positions closer to the power jet. Figures 21 and 22 show that the theory predicts larger velocities than those obtained experimentally. As the angle of radial position is increased, i.e. θ = 42 and 78 degrees, the agreement between the theoretical and experimental results is considerably improved. As a matter of fact, Fig. 26 shows that there is fairly good agreement between the two studies.

In conclusion, it can be stated that for a given Reynolds number, an increased setback will result in a more stable jet attachment to the boundary. Also an increased Reynolds number tends to stabilize the attachment for a given setback. This is evidenced by both the pressure and velocity profiles.

Of special interest is the finding that the magnitude of the parameter p_w/P_s is almost insensitive to Reynolds number, setback, and control port conditions. This is quite remarkable in view of the ranges of values investigated.

As predicted by Newman, on the basis of phenomenological considerations, the separation angle was relatively insensitive to Reynolds number within the range of Reynolds numbers investigated. But the fact that the separation angle was also relatively insensitive to the value of the setback and control port condition was wholly unexpected.

The foregoing discussion has been confined to setbacks of 0.025" and 0.075", although the experiments included an intermediate setback of 0.050". The data obtained with that particular setback, though not presented herein for the sake of brevity, have in every respect confirmed the conclusions advanced so far.

The ultimate purpose of the investigation reported herein was, as previously stated, the understanding of the mechanism which provided, in convex-walled vented amplifiers, pressure recoveries which are in excess of those obtained by one dimensional isentropic flow analysis. In order to account for the excess energy (per unit mass) recovered at the load port, beyond and above that provided by the source, the necessity of additional outputs, such as a vent and/or a splitter plate, at which the average energy per unit mass is lower than that at the input, has been recognized. The explanation of a convincing and experimentally verifiable mechanism required that: (a) there must be a Coanda wall along which the energy loss due to friction is relatively smaller than that along a straight Coanda wall: (b) the Coanda wall must be such that the resulting flow can rapidly undergo an energy redistribution with high energy flow concentrating near the core and the low energy flow at the two sides of the core; (c) the energy redistribution must be such that the energy per unit mass at the high-energy regions is higher than that at the input: and finally, (d) there must be two outputs (a vent and a splitter plate) to discharge or "skim off" the low energy flow.

A careful analysis of the velocity profiles (including those not presented herein) have shown that all of the requirements cited above are satisfied with a convex-walled vented amplifier and that the explanation of the excess-energy recovery mechanism lies in the distribution of the resulting velocities. In order to proceed with a systematic development of the understanding of the mechanism, we will first consider the free laminar and turbulent jets. Numerous analyses and experiments have shown that (see for example Schlichting's Boundary Layer Theory) in

two-dimensional laminar jets the center-line velocity decreases with distance from the nozzle as $x^{-1/3}$, and in two-dimensional turbulent jets as $x^{-1/2}$. The corresponding ratio for a circular jet is x^{-1} regardless of whether the jet is laminar or turbulent. Thus in a free jet u_m/U_o is always less than unity and decreases rapidly with distance. This conclusion is equally valid for the velocity profiles in a jet deflected by an inclined plate (7). Consequently, either in a free jet or in a jet deflected by an inclined plane wall, nowhere the energy per unit mass is greater than that at the input. In a flow along a convex wall, however, u_m/U_o first increases to about 1.25 and then decreases slowly to about 0.5 as the distance along the quadrant increases. Thus there is a region or central core in which the energy per unit mass is considerably larger (about 50% larger) than that in the nozzle. It should also be remembered that in the nozzle, where the flow is a fully developed turbulent flow, u_m/U_o is about 0.82. Consequently, the maximum velocity in the jet varies from 0.82 at the nozzle to about 1.2 as the jet proceeds along the curved wall. In order to take full advantage of the energy-redistribution and to direct the high energy flow into the load port before the ratio u_m/U_o begins to decrease, one must place the splitter plate as close as possible to the nozzle (without making the jet unstable), drain the low energy flow near the wall through the vent, and finally, deflect away from the load port the low energy flow at the upper portion of the jet by means of the splitter plate. It is in this sense that the splitter plate skims off from the top of the jet, the low energy flow and serves as a "skimmer plate" rather than as a "splitter plate", (See Fig. 27). The resulting process may be regarded as the selective withdrawal of the high energy flow from

the load port (See Fig. 28).

As far as the effect of the control port condition is concerned, it is clear from the velocity profiles that it has very little influence on the energy recovery of the amplifier. Thus the explanation of the mechanism of obtaining high pressure recoveries lies in the concentration of high energy flow in the central core of the deflected jet and in the withdrawal of the low energy by means of vents and the splitter plate. The same process does not occur in the straight-walled amplifiers because nowhere in the velocity profile along the wall u_m/U_o exceeds unity (7).

A theoretical analysis of the turbulent flow along a circular arc through the use of a suitable mixing length hypothesis and the reasons for the attainment of velocity ratios u_m/U_o larger than unity will be presented in the near future.

REFERENCES

1. Sarpkaya, T., "Characteristics of Load-Insensitive Bistable Fluid Amplifiers with Convex and Concave Coanda Walls", NU-Hydro-Report No. 033-TS, July 1967.

2. Sarpkaya, T. and Kirshner, J. M., "The Comparative Performance Characteristics of Vented and Unvented, Cusped, and Straight and Curved-Walled Bistable Amplifiers", Proceedings of the Third Cranfield Fluidics Conference, Turin, Paper F3, May 1968, pp: 3-37 to 3-48.

3. Publishing House of the Academy of Sciences, USSR, Automatics and Telemechanics, Vol. XXIV, No. 8, August 1963, pp: 1155-1162.

4. Curtiss, H. A. and Liquornik, D. J., "Research Studies in Proportional Fluid State Control Components", Giannini Controls Corporation Report, September 1963.

5. Curtiss, H. A., Feil, O. G., Liquornik, D. J., "Separated Flow in Curved Channels with Secondary Injection", Giannini Controls Corporation Report, May 1964.

6. Kadosch, M., "Attachment of a Jet to a Curved Wall", Proceedings of the 2nd Fluid Amplification Symposium, Vol. IV, May 1964.

7. Newman, B. G., "The Deflection of Plane Jets by Adjacent Boundaries - Coanda Effect", Boundary Layer and Flow Control - Its Principles and Application, edited by G. V. Lachman, Vol. I, Pergamon Press, 1961.

8. McGlaughlin, D. W. and Greber, I., "Experiments on the Separation of a Fluid Jet from a Curved Surface", Advances in Fluidics, ASME, 1967, pp: 14-30.

9. Bailey, A. B., "Use of the Coanda Effect for the Deflection of Jet Sheets Over Smoothly Curved Surfaces", Univ. of Toronto Institute of Aerophysics TN 49 (1961).

10. Von Glahn, V. H., "Use of the Coanda Effect for Obtaining Jet Deflection and Lift with Multiple Flat-Plate and Curved-Plate Deflection Surfaces", NACA TN 4377 (1958).

11. Mehus, T., "An Experimental Investigation into the Shape of Thrust Augmentation Surfaces in Conjunction with Coanda-Deflected Jet Sheets (Part-II)", Univ. of Toronto, UTIA TN 79 (1965).

12. Von Karman, T., "Theoretical Remarks on Thrust Augmentation, Reissner Anniversary Volume", Contributions to Applied Mechanics (J. W. Edwards, Ann Arbor, Mich., 1949), pp: 461-468.

13. McKinney, M. O., "NACA Research on VTOL and STOL Aeroplanes", Reprint from the Sixt Anglo-American Aeronautical Conference, 1957, pp: 201-232.

14. Liepmann, H. W. and Laufer, J., "Investigations of Free Turbulent Mixing", NACA TN 1257, 1947.

15. Lighthill, M. J., "Notes on the Deflection of Jets by Insertion of Curved Surfaces and on the Design of Bends in Wind Tunnels", ARC R & M. No. 2105, 1945.

16. Metral, A., "Sur un Phénomène de Déviation des Veines Fluides et ses Applications. Effet Coanda, Cabinet Technique du Ministere de l'air, 1938.

17. Metral, A. and Zerner, F., "L'Effet Coanda", Publication Scientifiques et Techniques du Ministère de L'air, No. 218, 1948; M.O.S., TIB/T4027, 1953.

18. Yen, K. T., "An Investigation of the Coanda Effect for Supersonic Flows", Rensselaer Polytechnic Institute, TR AE5405, March 1954.

19. Görtler, H., "Berechnung von Aufgaben der freien Turbulenz auf Grund eines neuen Naherungsansatzes", Z. Angew. Math. Mech., 22, 244, 1942.

20. Glauert, M. B., "The Wall Jet", J. Fluid Mech., 1, 625, 1956.

21. Reichardt, H., "On a New Theory of Free Turbulence", J. Roy. Aero. Soc., 47, 167, 1943.

22. Förthmann, E., "Uber turbulente Strahlausbreitung", Ing.-Arch., 5, 42, 1934; NACA TM 789, 1936.

23. Sigalla, A., "Measurements of Skin Friction in a Plane Turbulent Wall Jet", J. Roy. Aero. Soc., 62, 873, 1958.

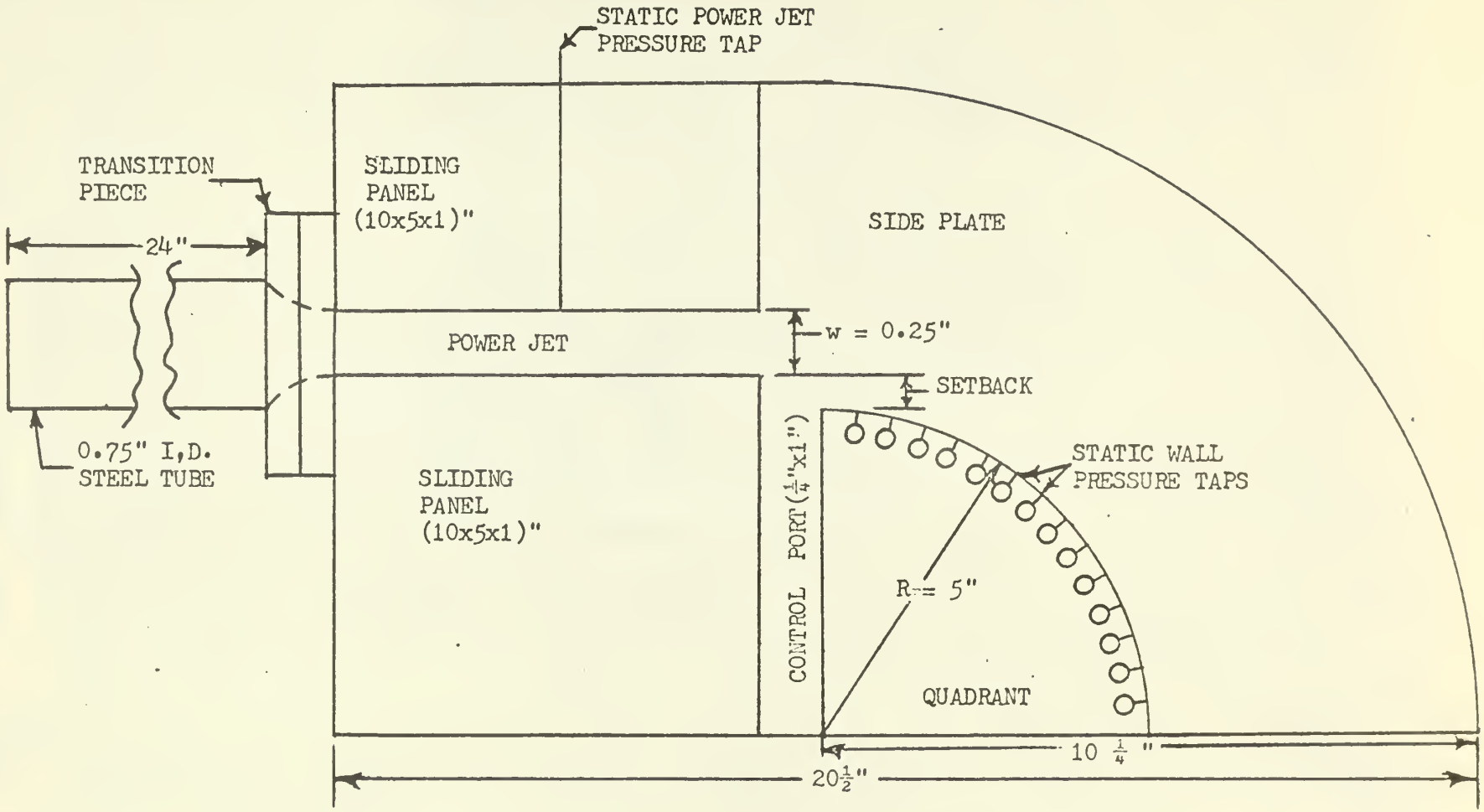

FIGURE 2. SCHEMATIC OF TEST SECTION

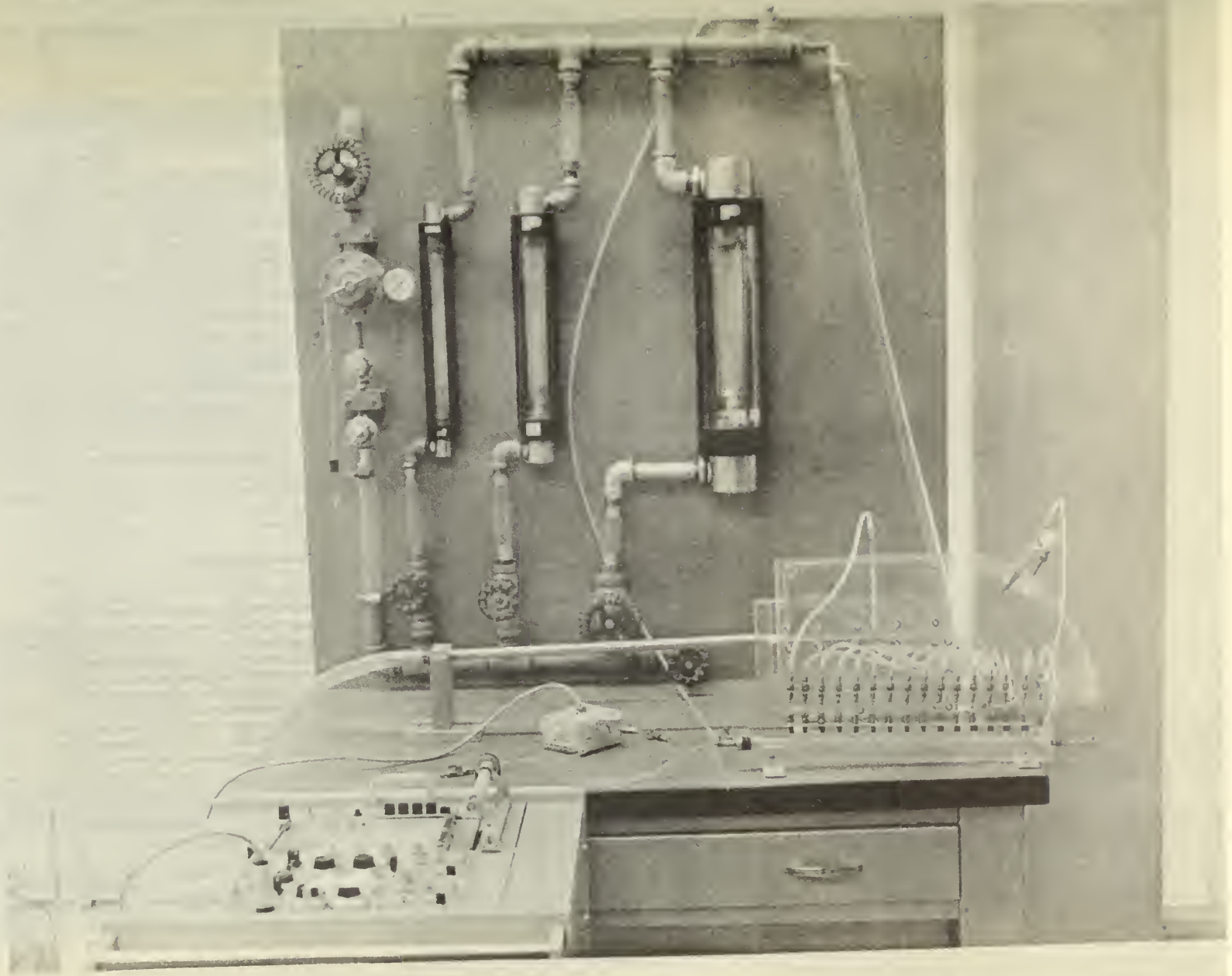

FIGURE 3 EXPERIMENTAL EQUIPMENT

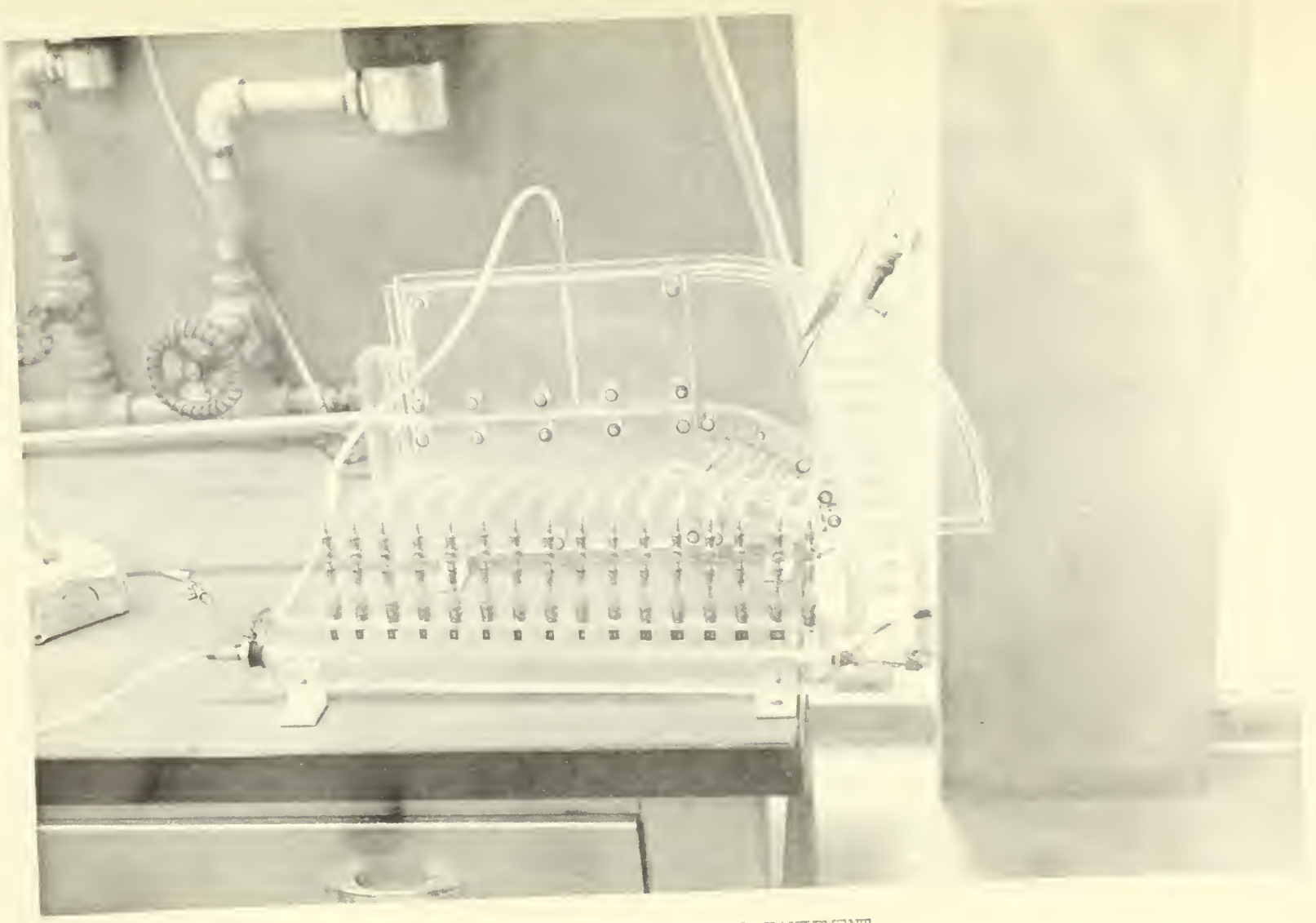

FIGURE 4 EXPERIMENTAL EQUIPMENT

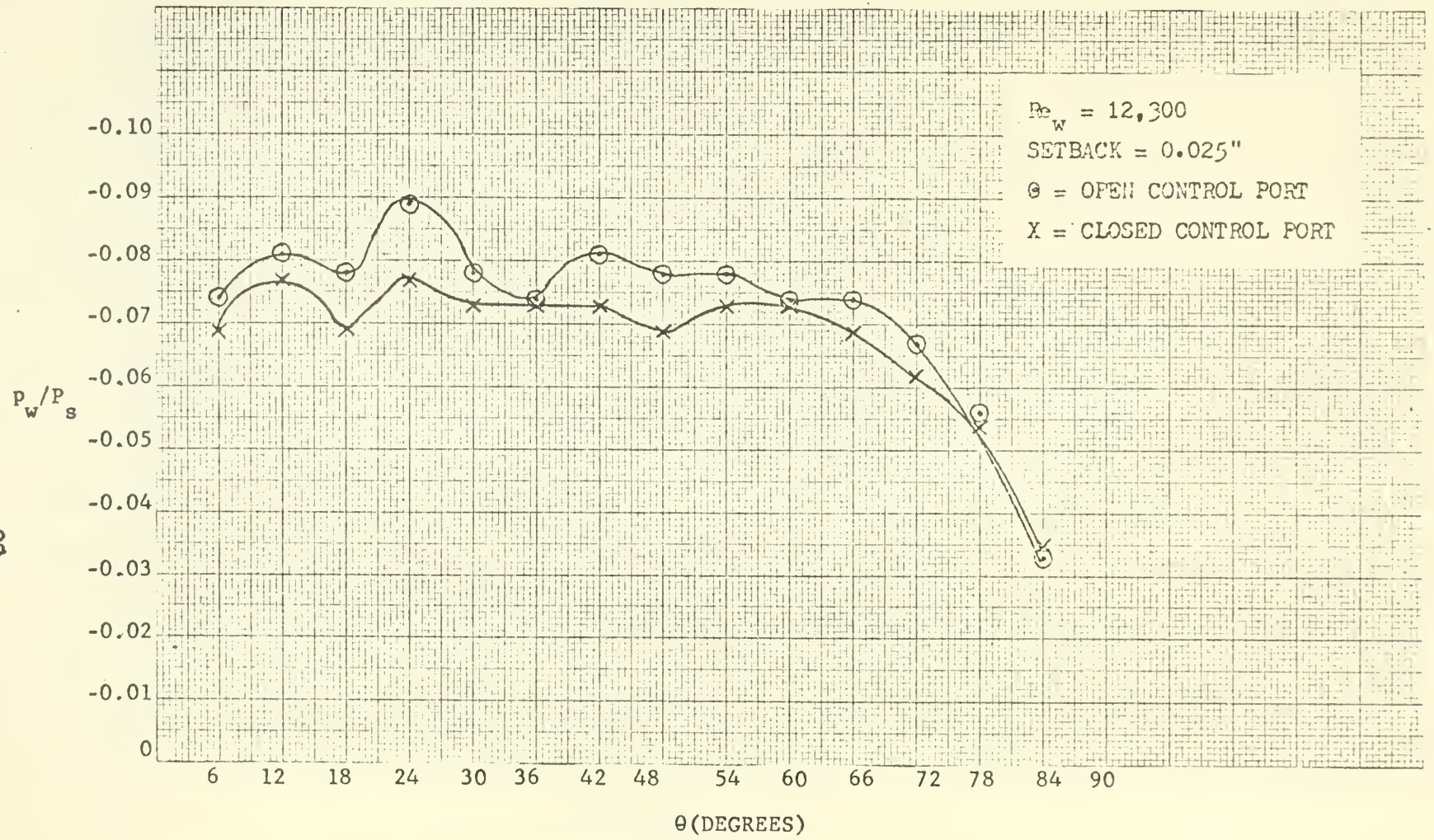

FIGURE 5. NORMALIZED QUADRANT PRESSURE PROFILE

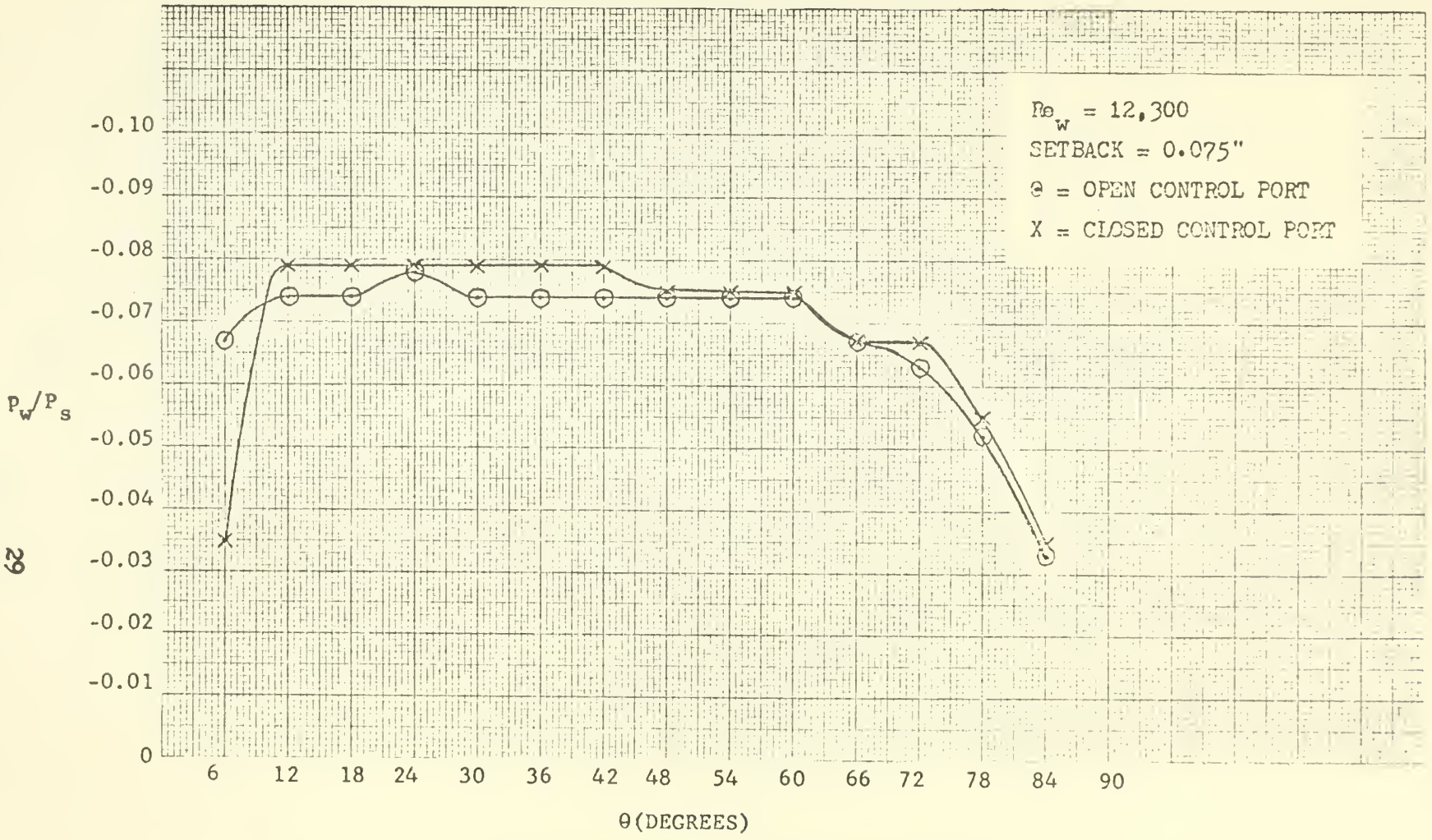

FIGURE 6. NORMALIZED QUADRANT PRESSURE PROFILE

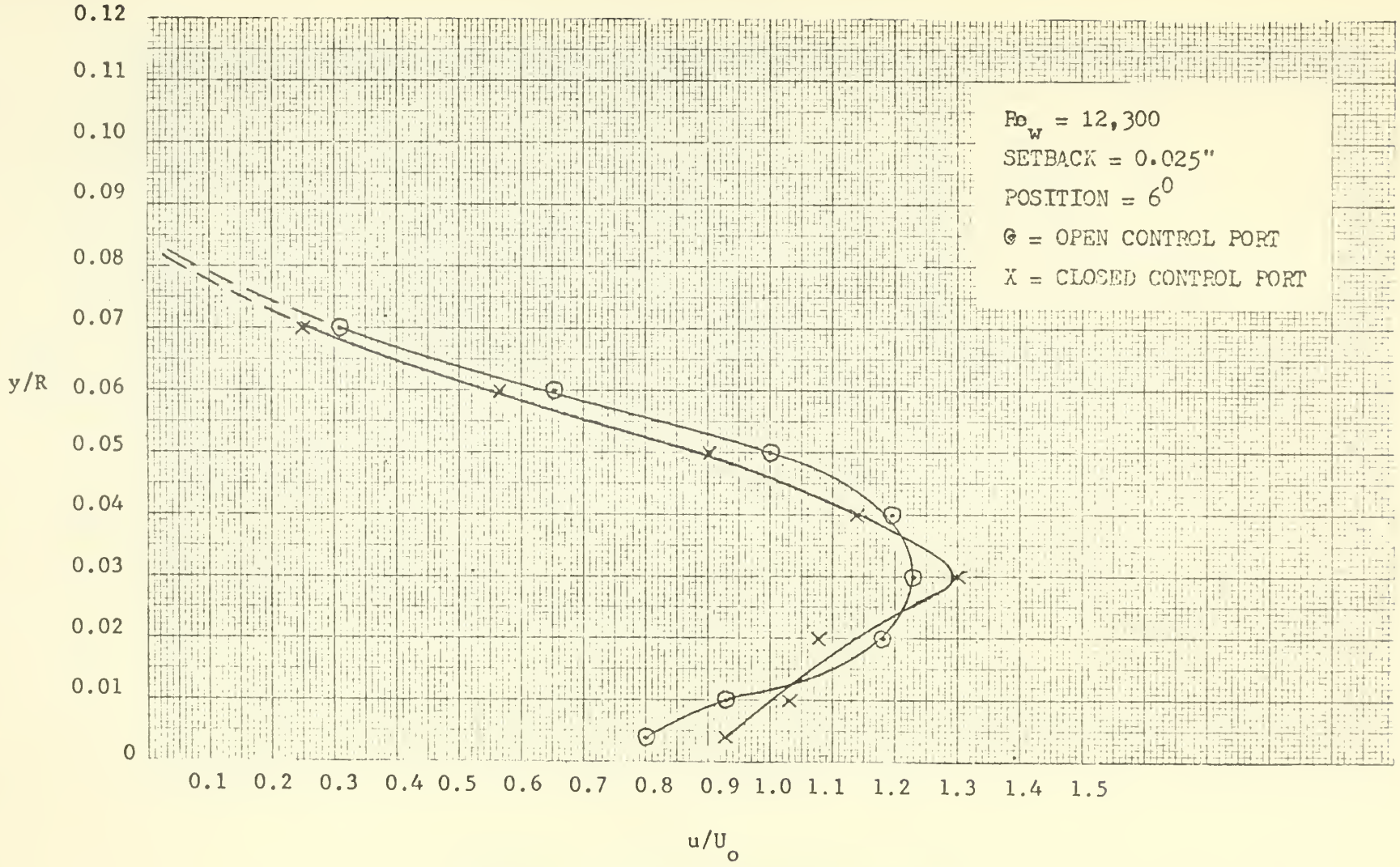

FIGURE 7. NORMALIZED VELOCITY PROFILE

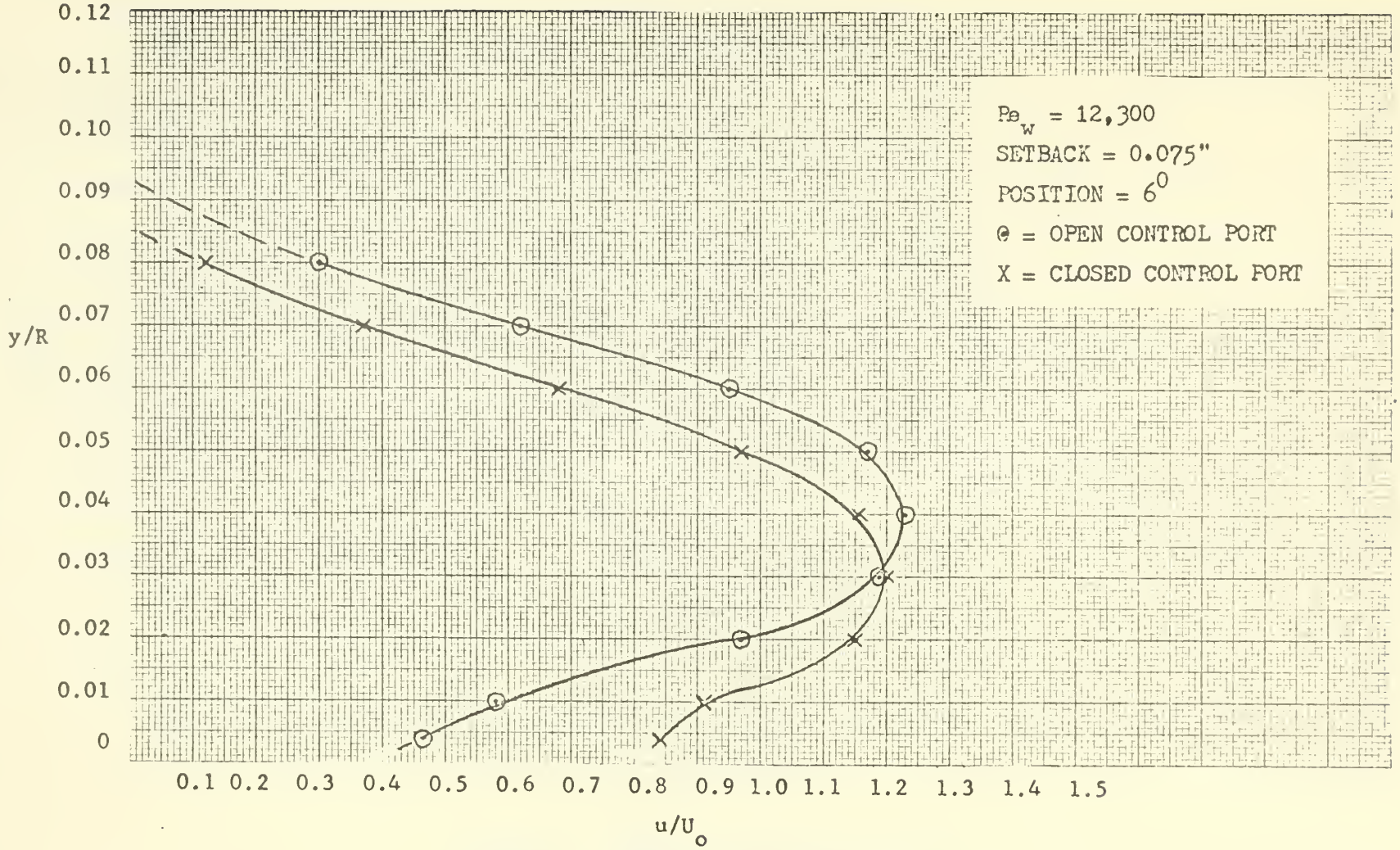

FIGURE 8. NORMALIZED VELOCITY PROFILE

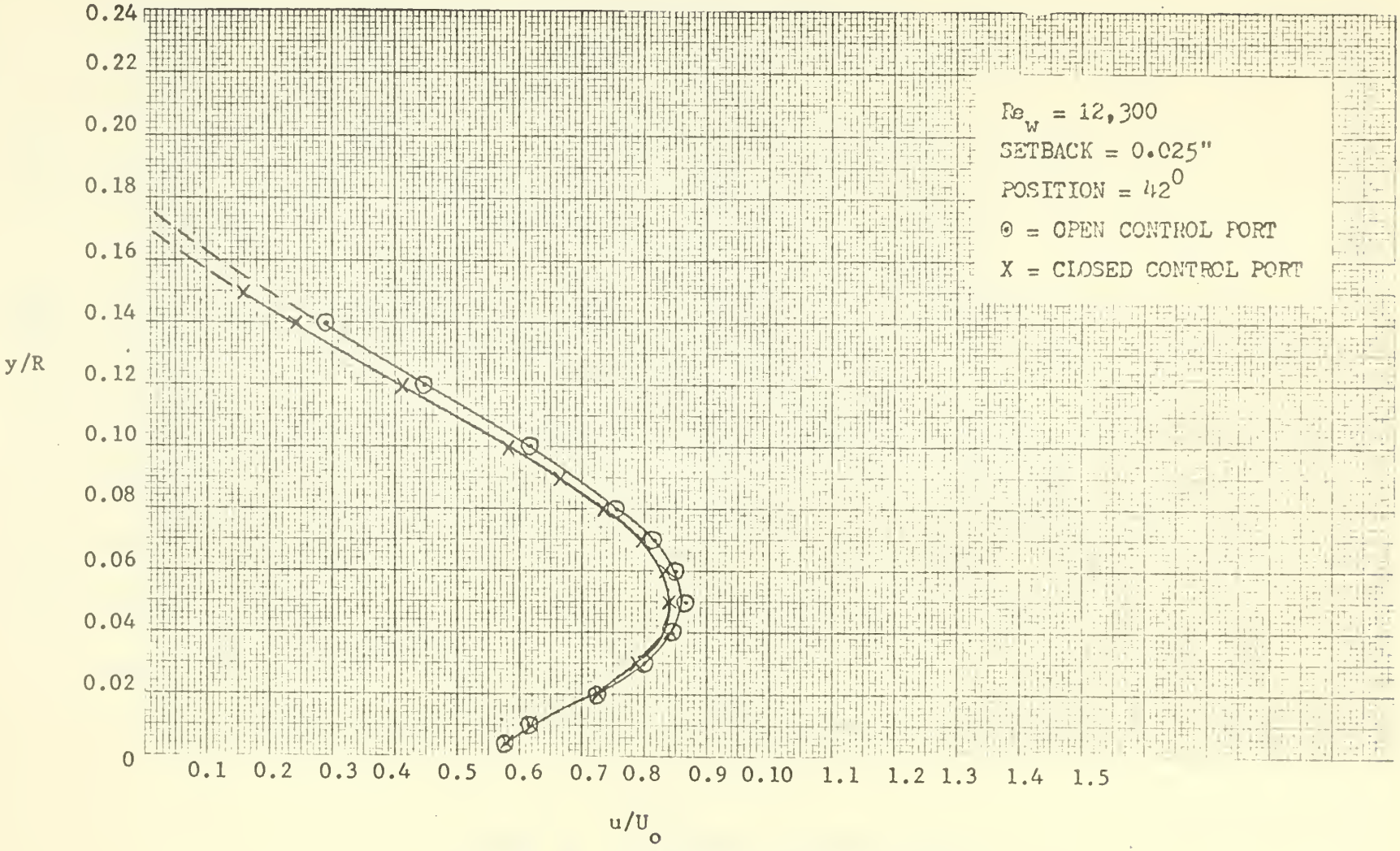

FIGURE 9. NORMALIZED VELOCITY PROFILE

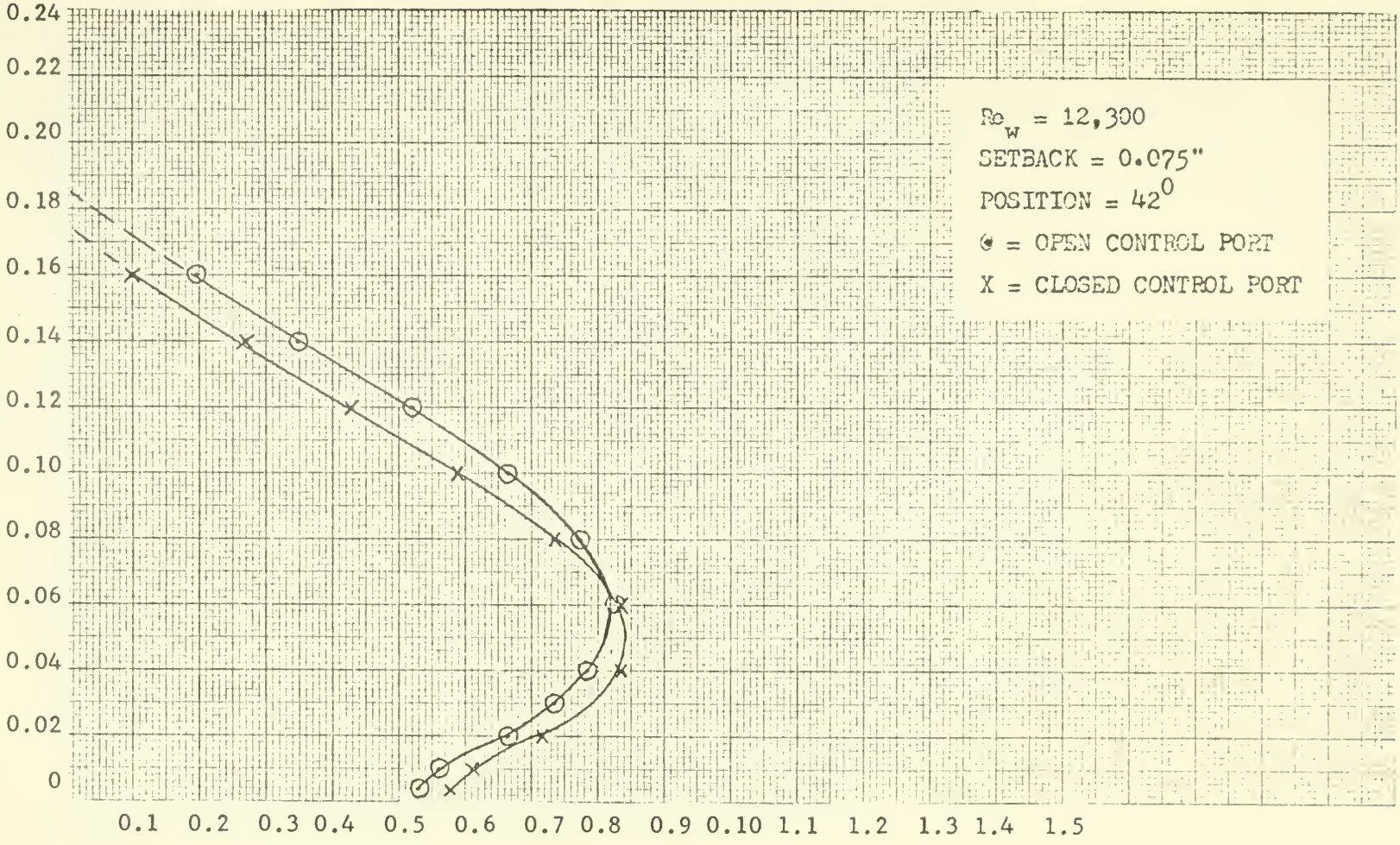

FIGURE 10. NORMALIZED VELOCITY PROFILE

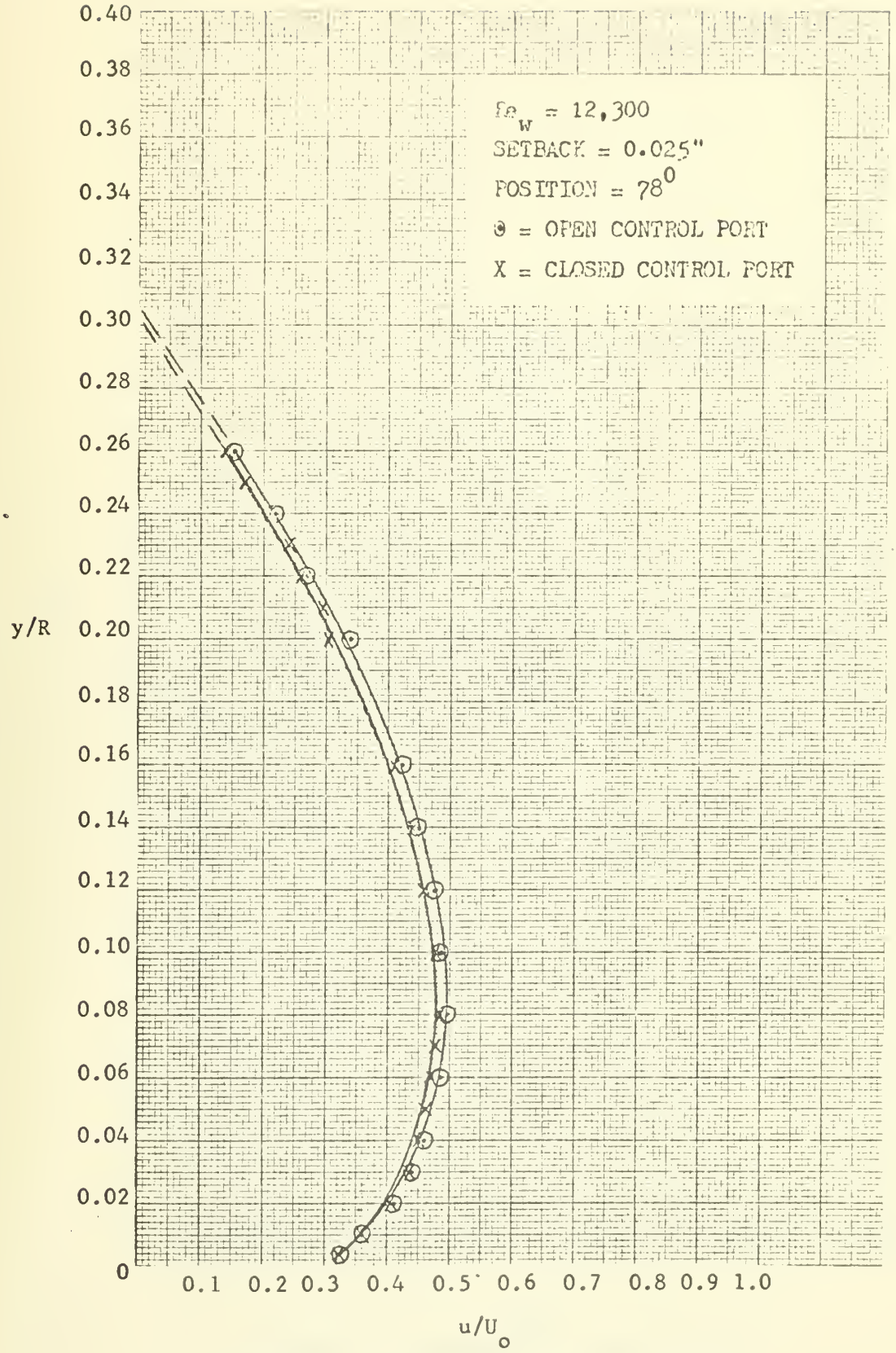

FIGURE 11. NORMALIZED VELOCITY PROFILE

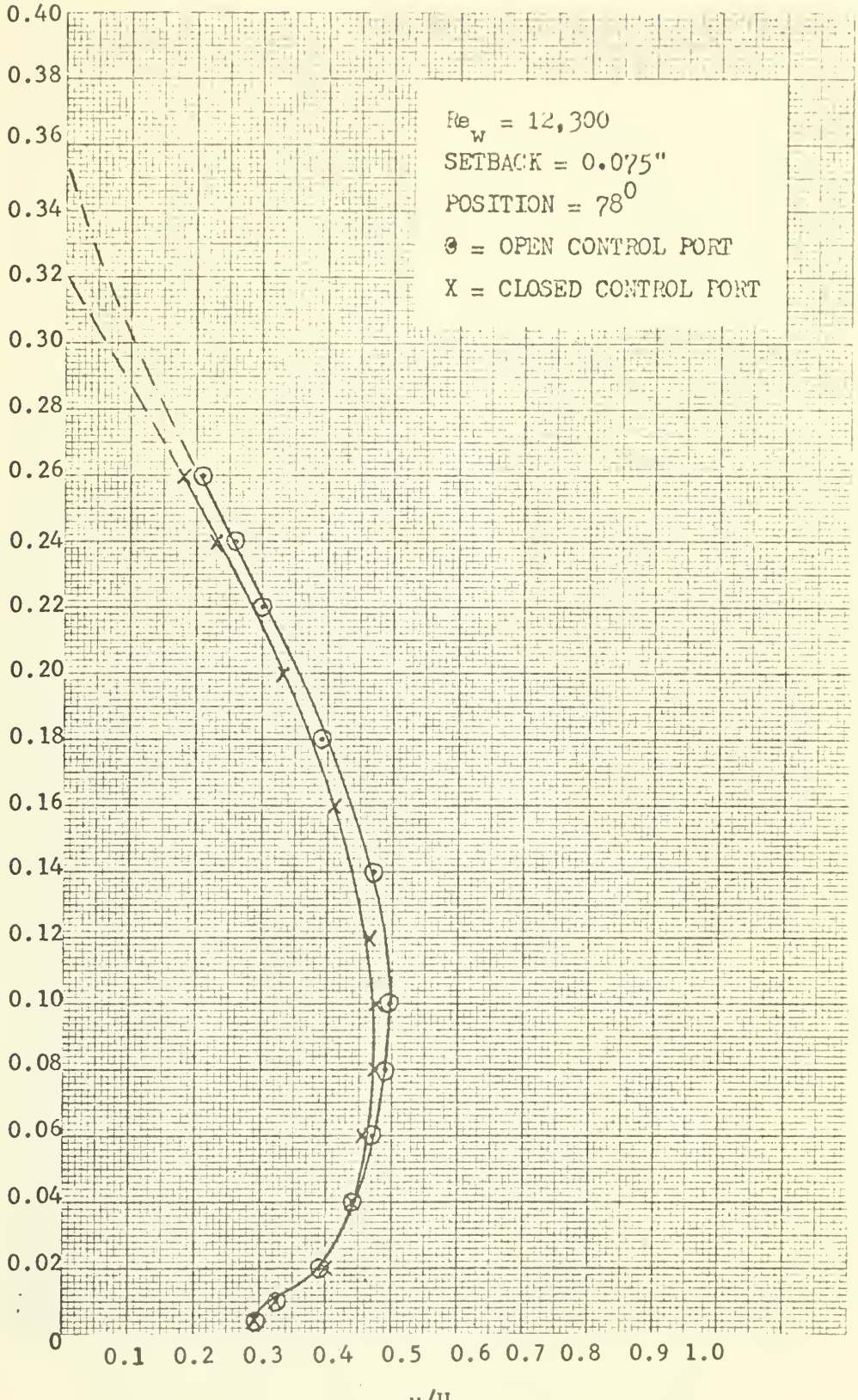

FIGURE 12. NORMALIZED VELOCITY PROFILE

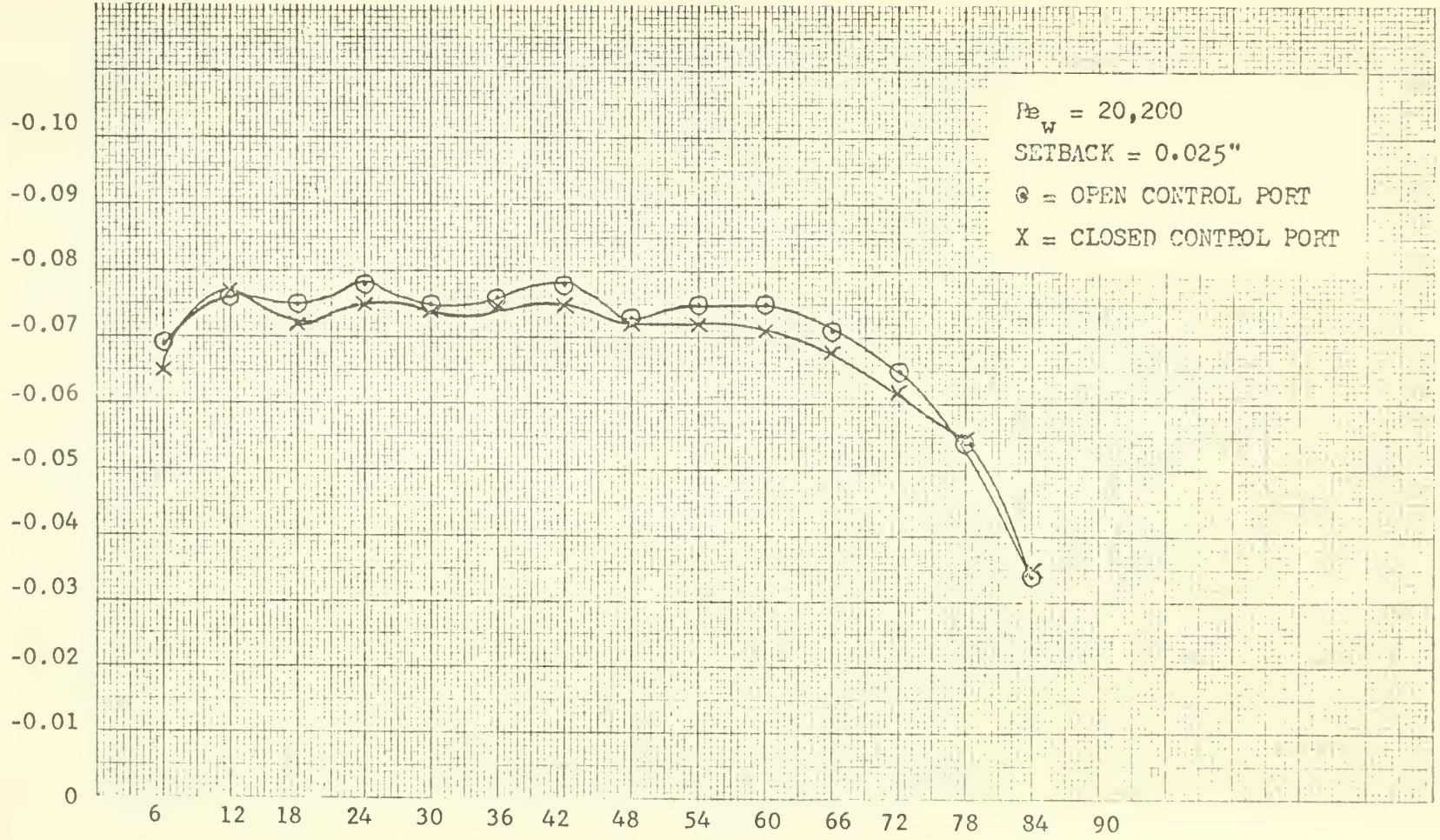

FIGURE 13. NORMALIZED QUADRANT PRESSURE PROFILE

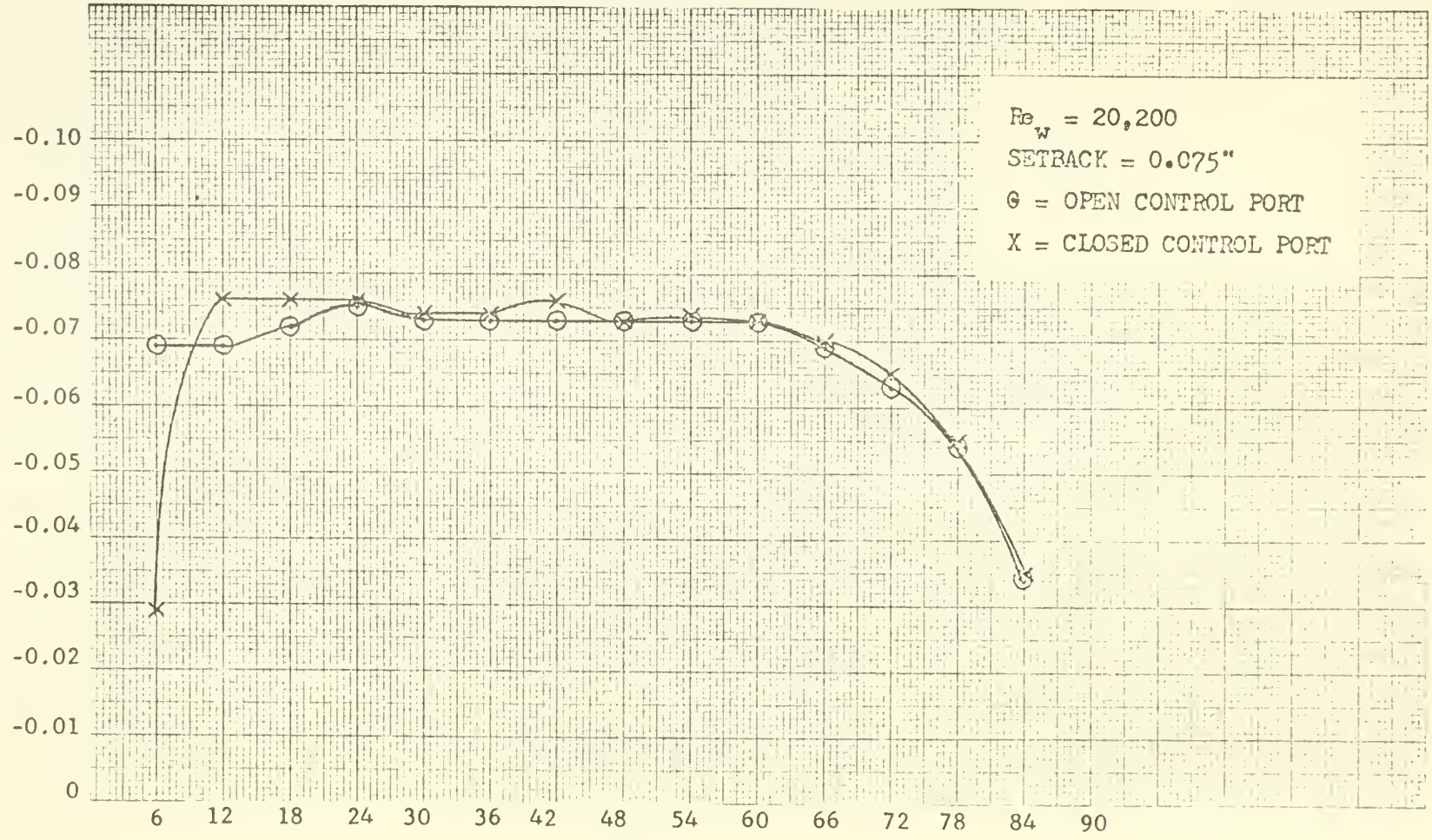

FIGURE 14. NORMALIZED QUADRANT PRESSURE PROFILE

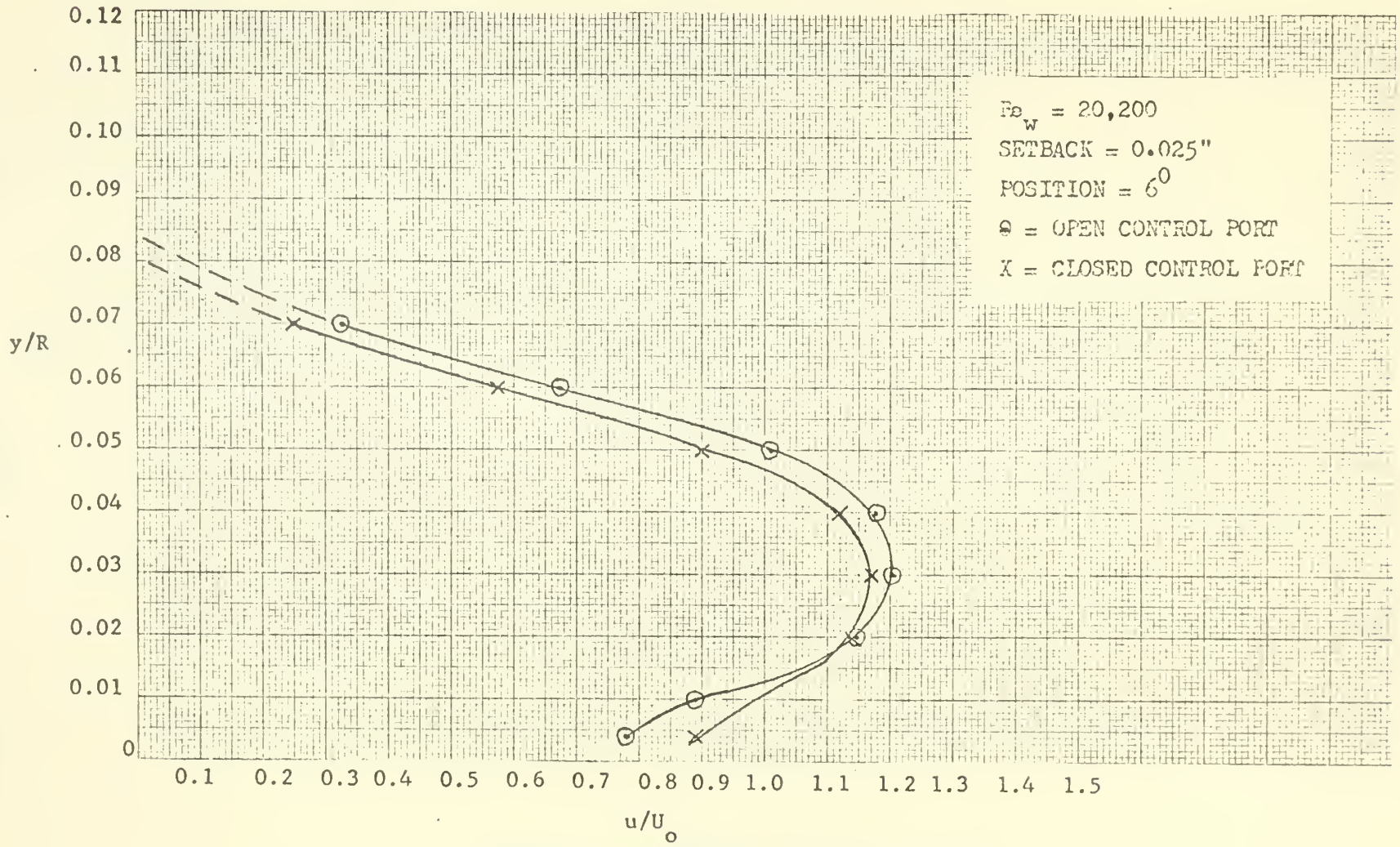

FIGURE 15. NORMALIZED VELOCITY PROFILE

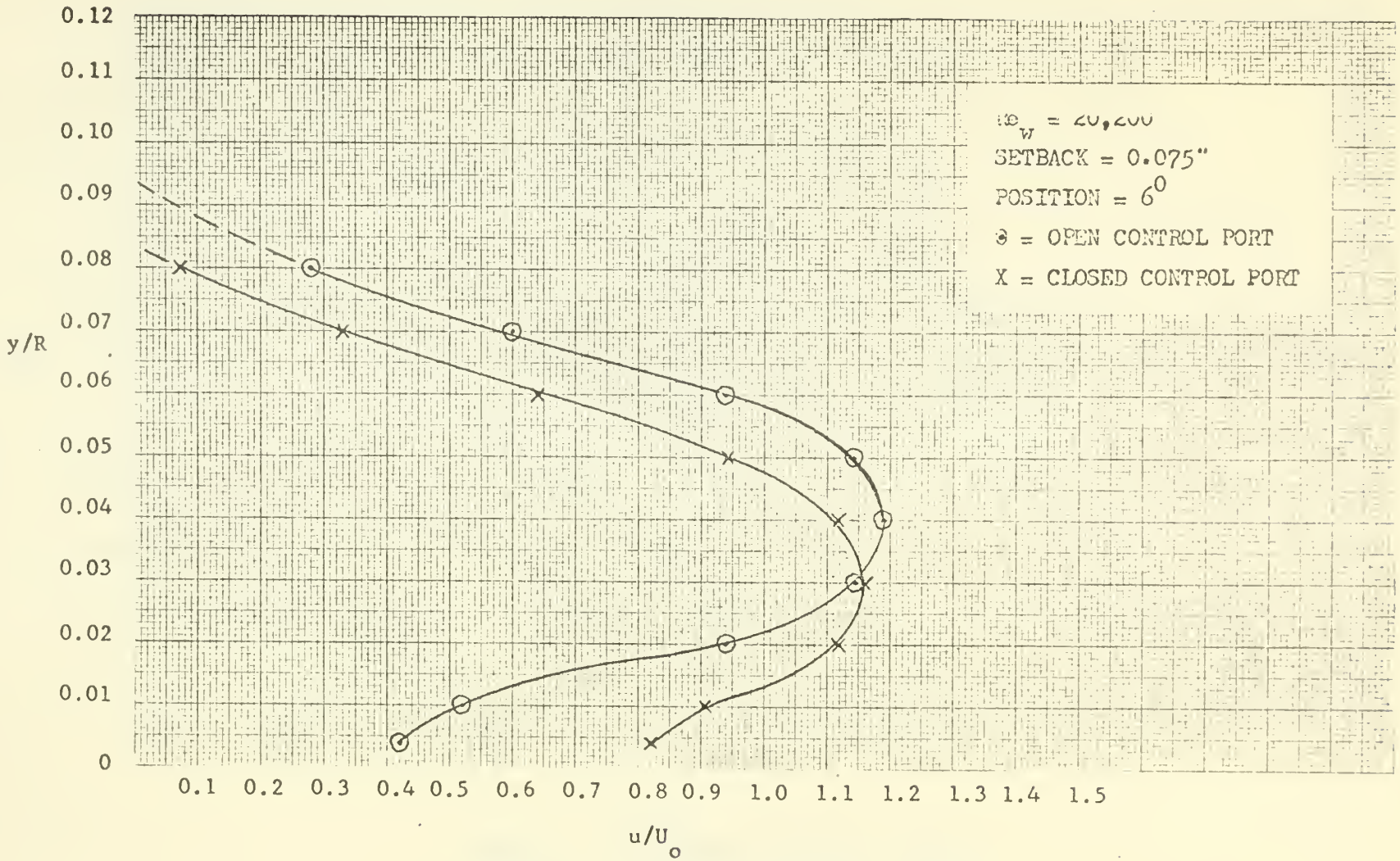

FIGURE 16. NORMALIZED VELOCITY PROFILE

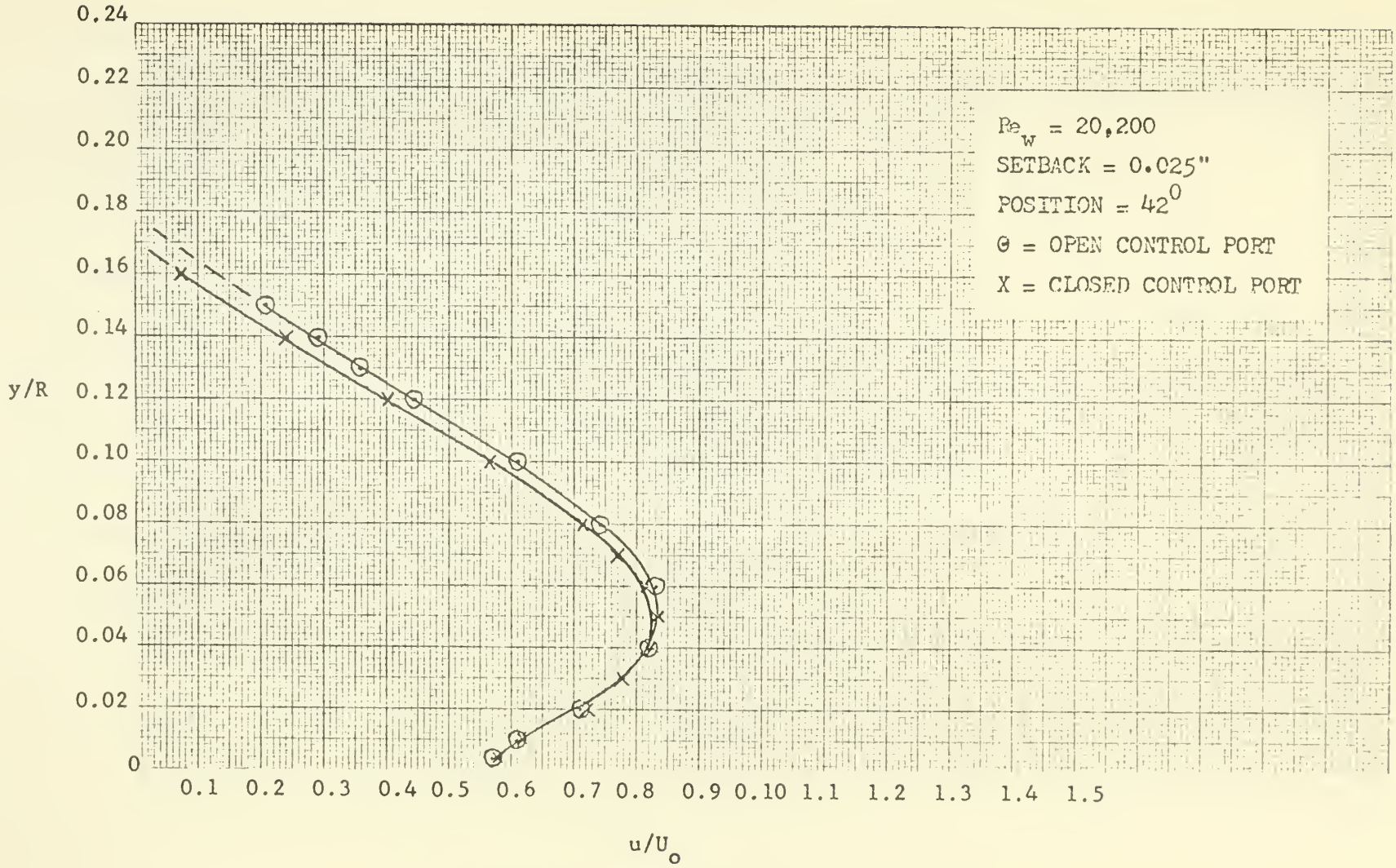

FIGURE 17. NORMALIZED VELOCITY PROFILE

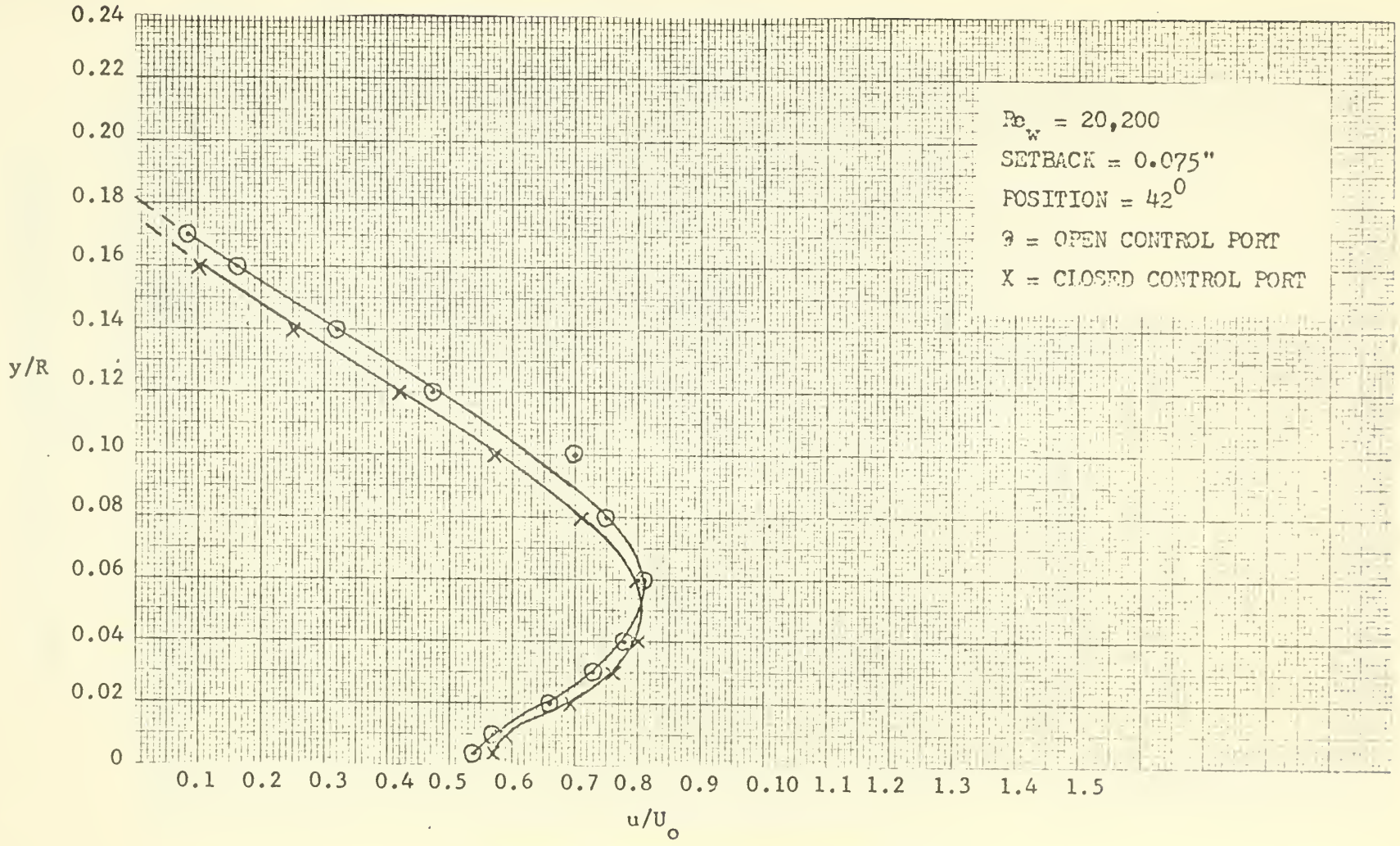

FIGURE 18. NORMALIZED VELOCITY PROFILE

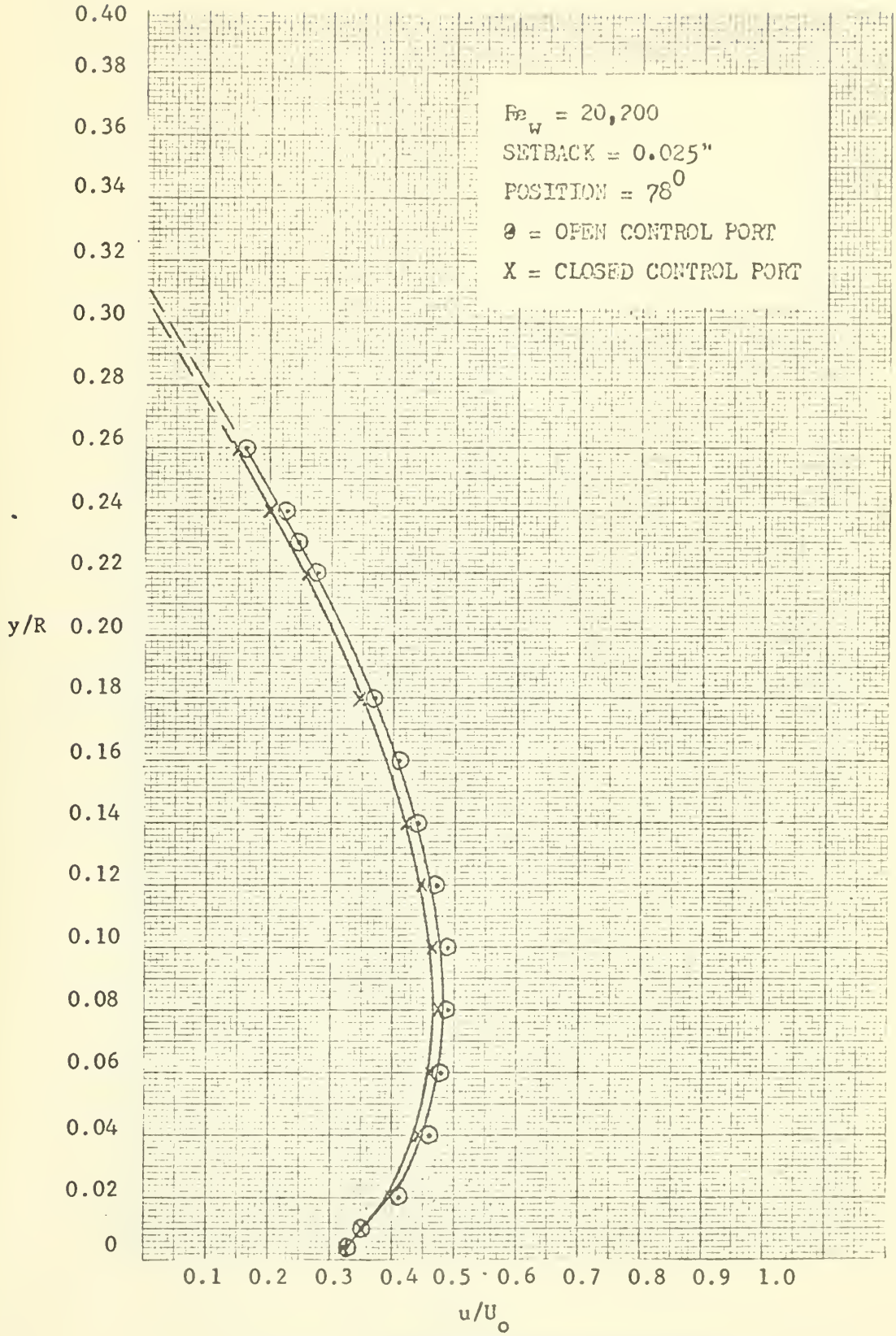

FIGURE 19. NORMALIZED VELOCITY PROFILE

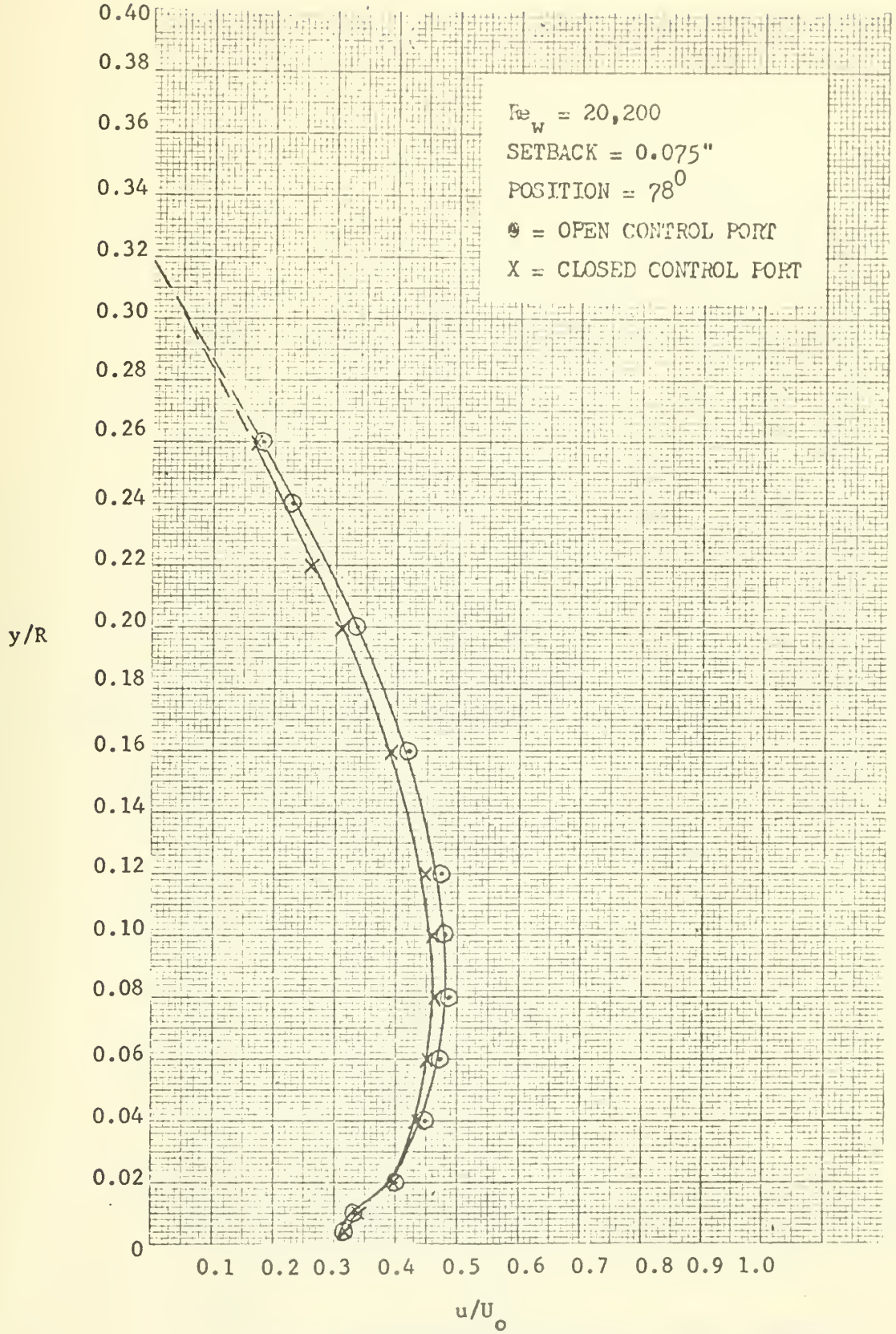

FIGURE 20. NORMALIZED VELOCITY PROFILE

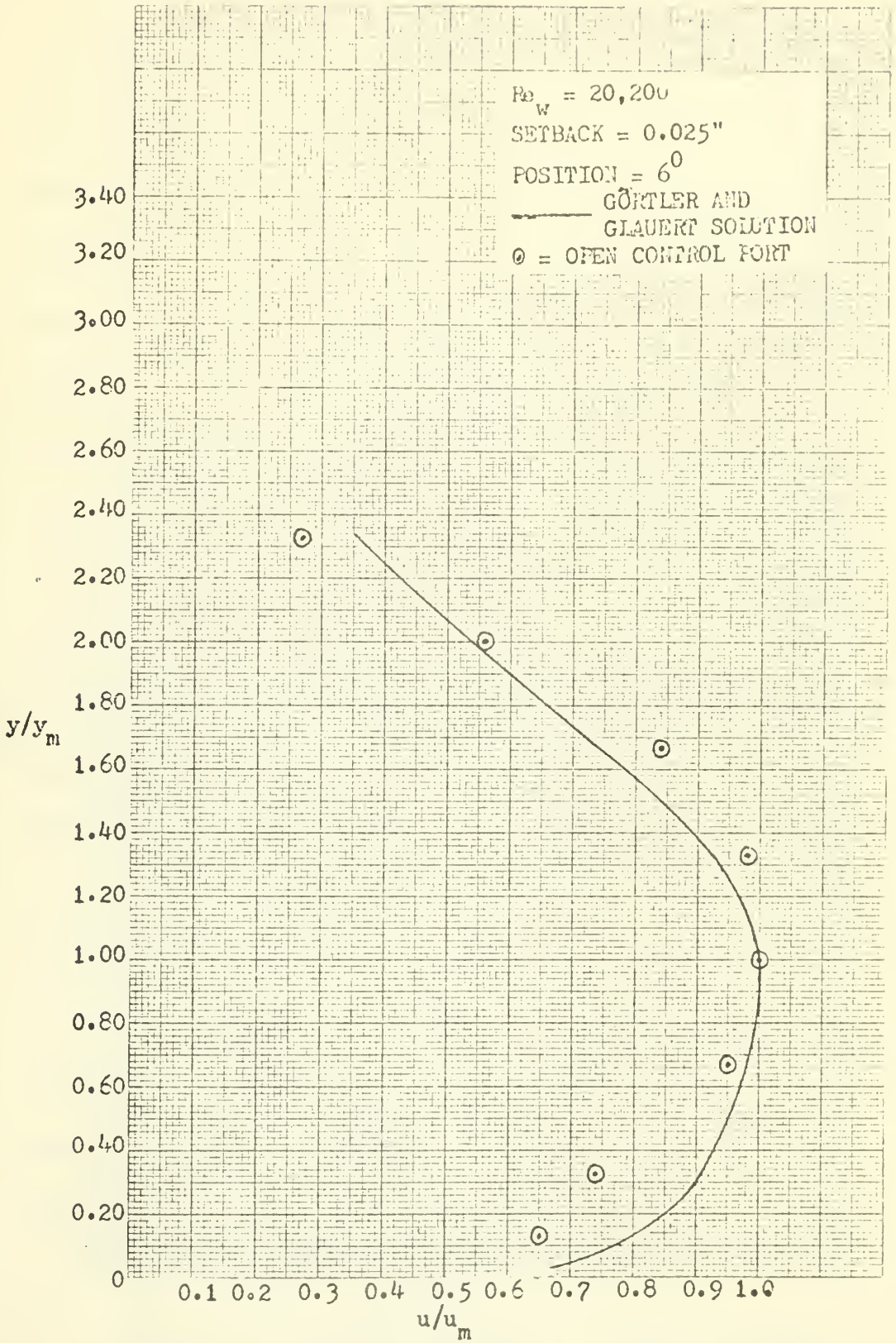

FIGURE 21. COMPARISON OF GÖRTLER - GLAUERT SOLUTION WITH EXPERIMENTAL DATA

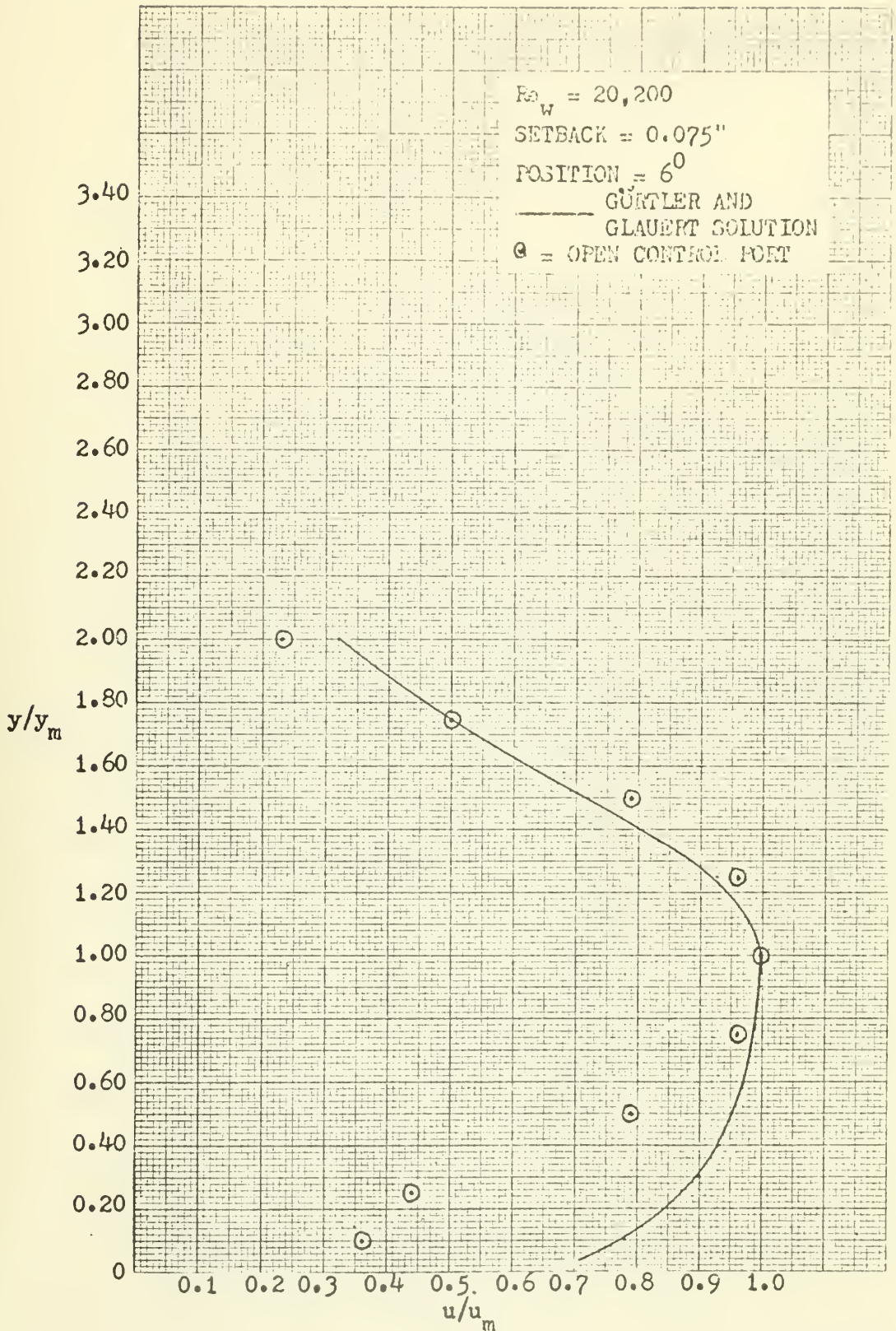

FIGURE 22. COMPARISON OF GÖRTLER - - GLAUERT SOLUTION WITH EXPERIMENTAL DATA

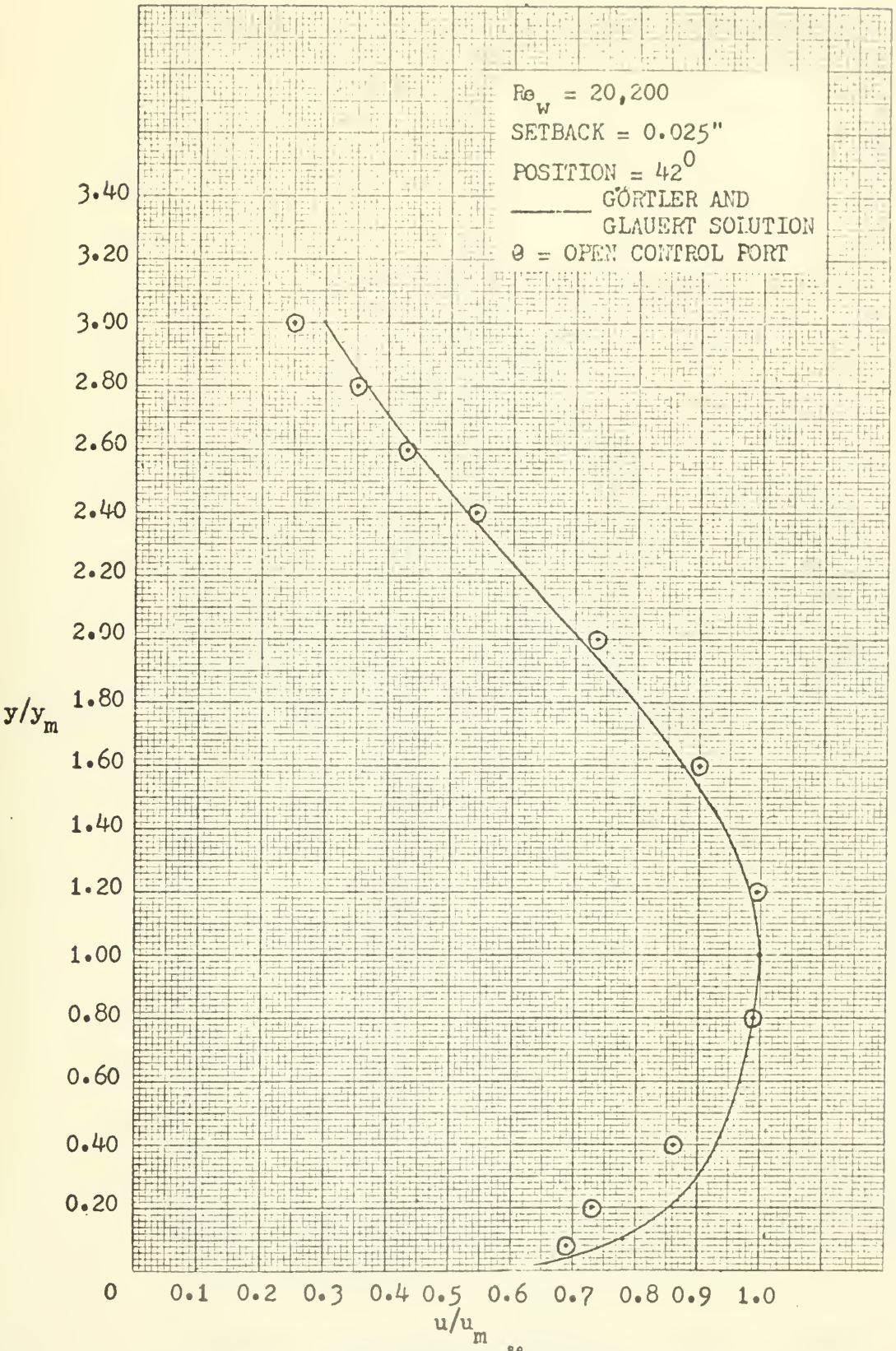

FIGURE 23. COMPARISON OF GÖRTLER - GLAUERT SOLUTION WITH EXPERIMENTAL DATA

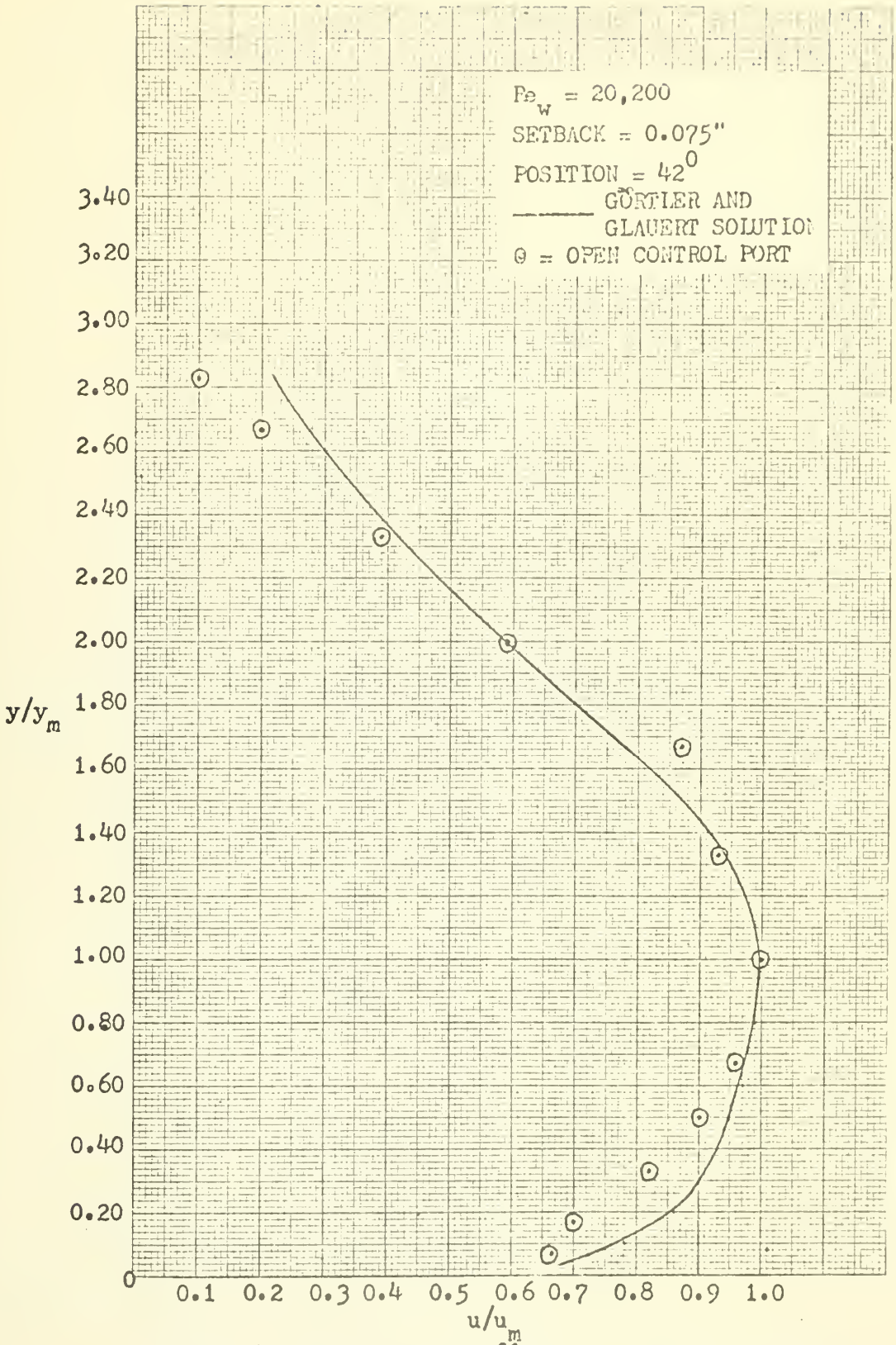

FIGURE 24. COMPARISON OF GÖRTLER - GLAUERT SOLUTION WITH EXPERIMENTAL DATA

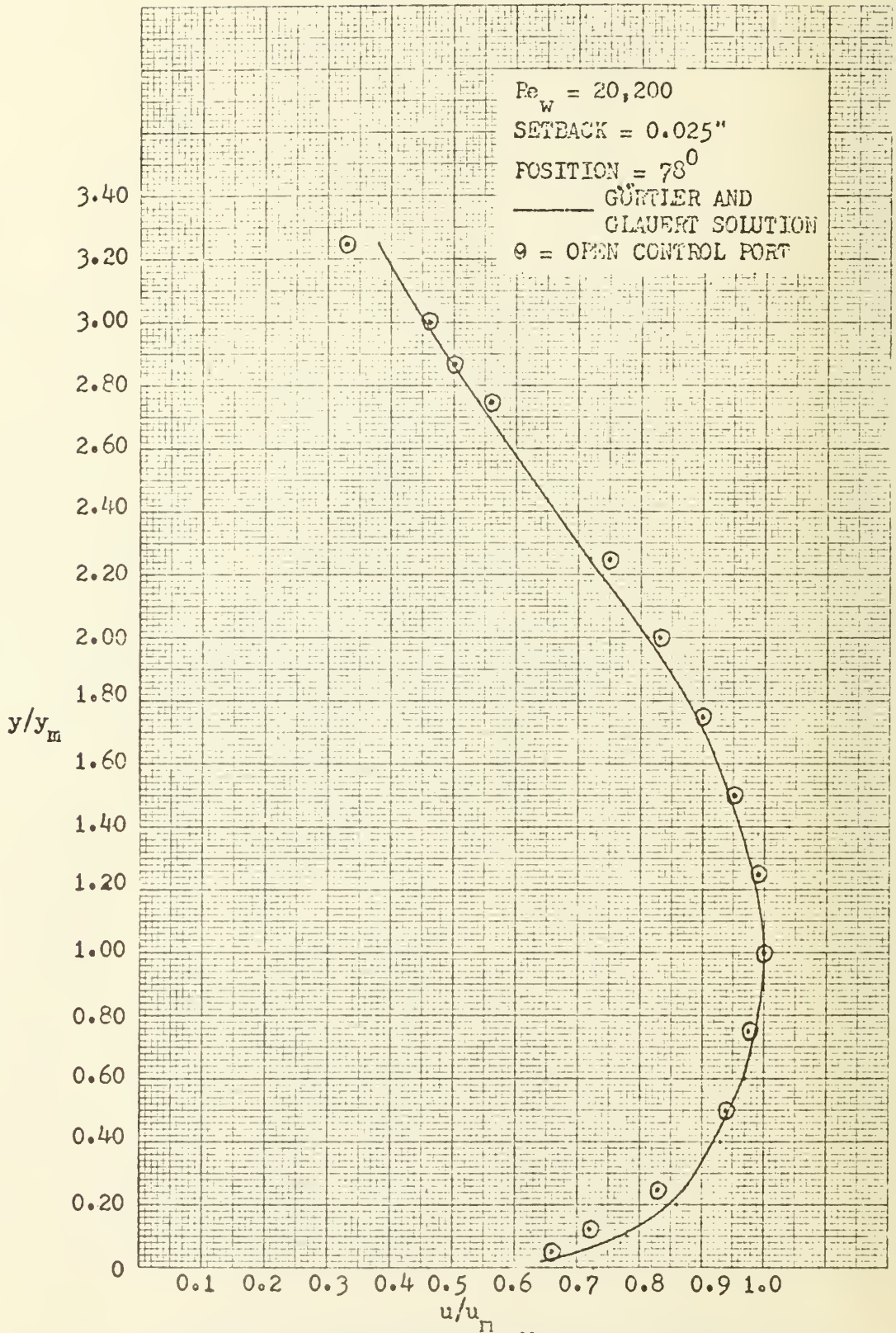

FIGURE 25. COMPARISON OF GÜRTLER - GLAUERT SOLUTION WITH EXPERIMENTAL DATA

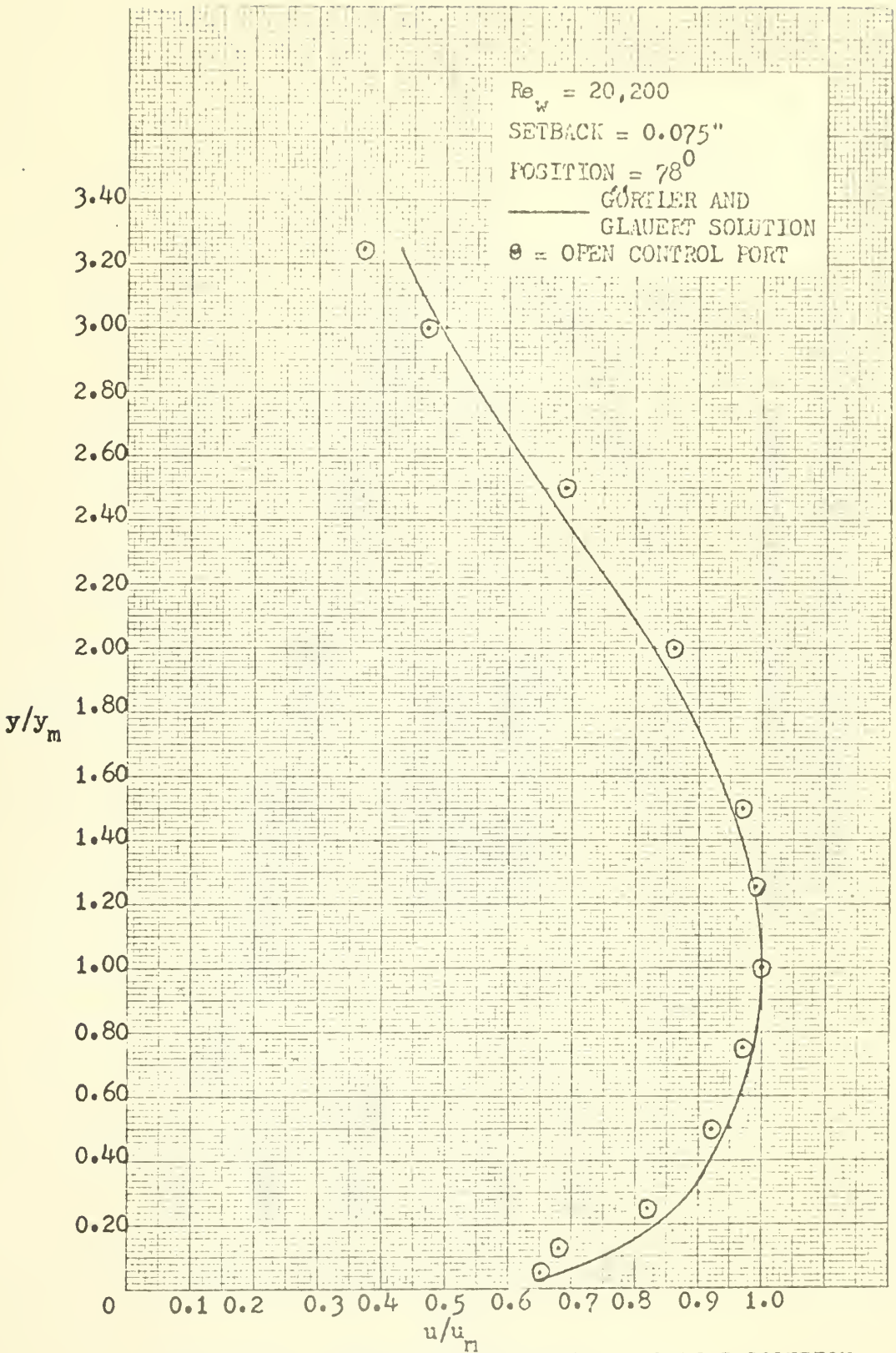

FIGURE 26. COMPARISON OF GÖRTLER - GLAUERT SOLUTION WITH EXPERIMENTAL DATA

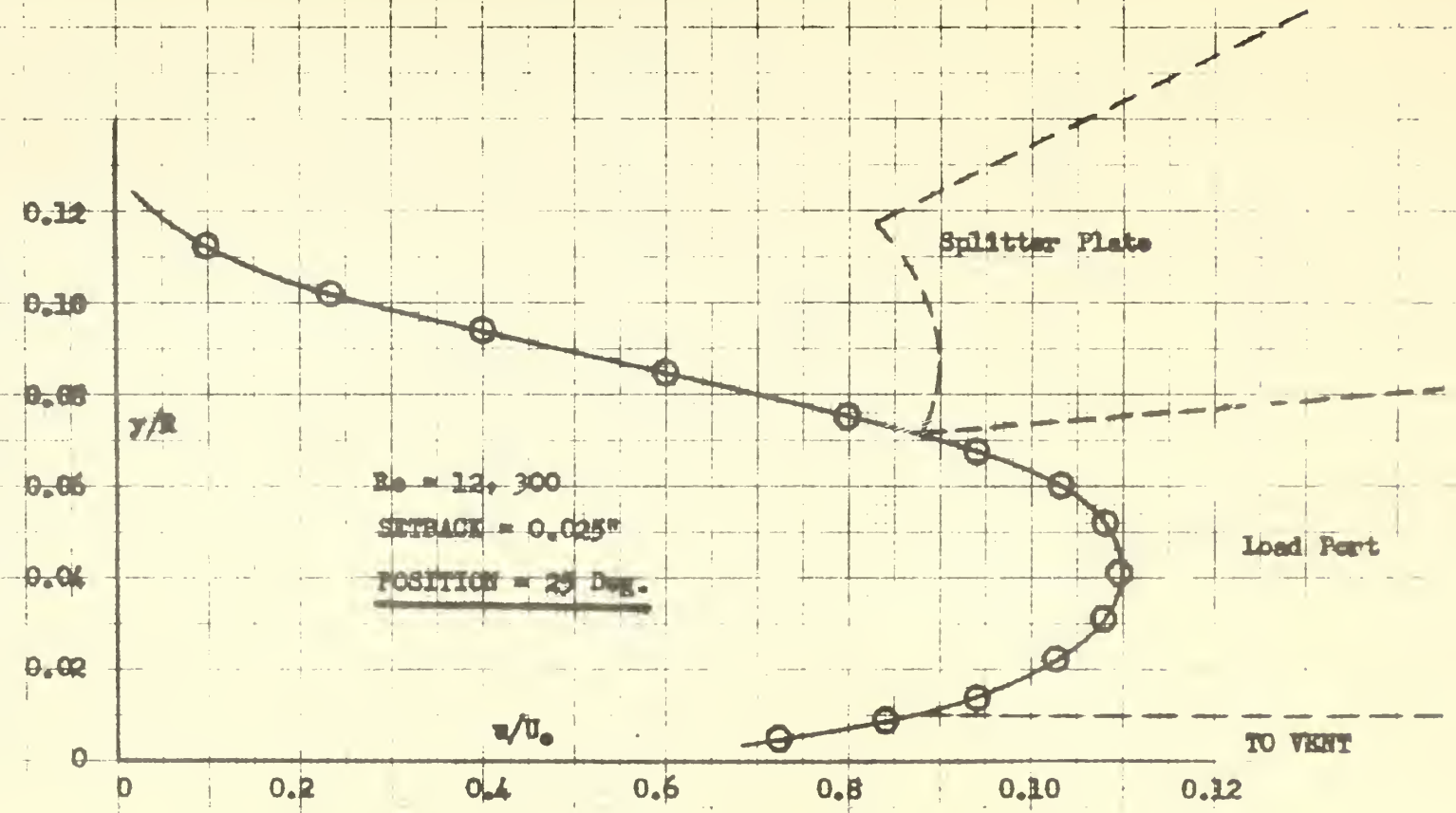

FIGURE 27 NORMALIZED VELOCITY PROFILE

AT THE ENTRANCE TO THE LOAD PORT (See Fig. 25)

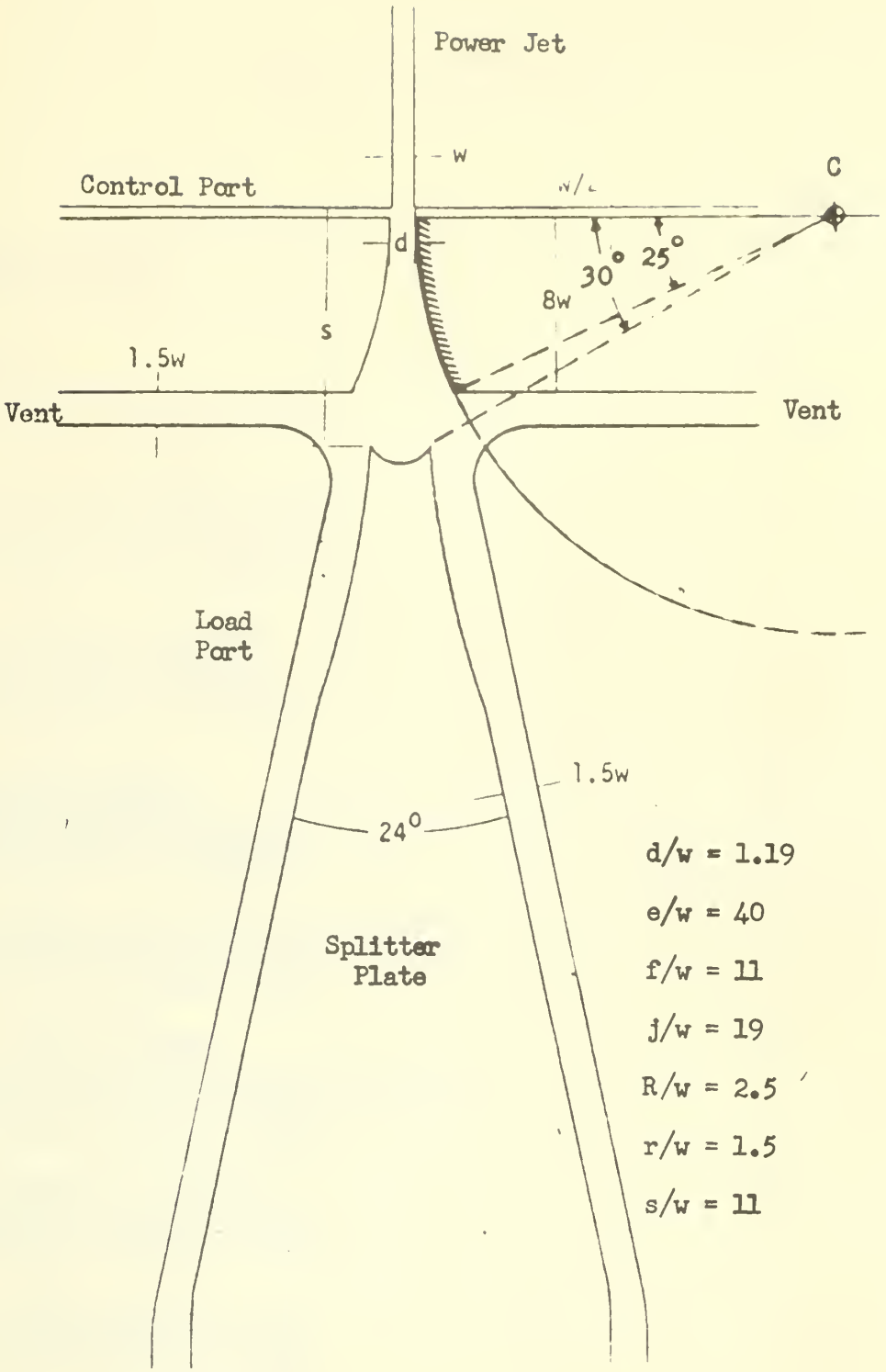

FIGURE 28 CONVEX-WALLED AMPLIFIER
(See References No. 1 and No. 2)

INITIAL DISTRIBUTION LIST

		No. Copies
1.	Defense Documentation Center Cameron Station Alexandria, Virginia 22314	20
2.	Library Naval Postgraduate School Monterey, California 93940	2
3.	Contracting Officer Harry Diamond Laboratories U. S. Army Materiel Command Washington, D. C. 20438	6
4.	Mr. Joseph M. Kirshner, Chief Fluid Systems Division Harry Diamond Laboratories Washington, D. C. 20438	2
5.	Mr. Raymond Keto Research Engineer Harry Diamond Laboratories Washington, D. C. 20438	2
6.	Department of Mechanical Engineering Naval Postgraduate School Monterey, California 93940	2
7.	Dr. Turgut Sarpkaya Department of Mechanical Engineering Naval Postgraduate School Monterey, California 93940	20
8.	Dean Robert F. Rinehart Naval Postgraduate School Monterey, California 93940	4
9.	CDR. Kevin O'toole Naval Postgraduate School Monterey, California 93940	2

Unclassified

Security Classification

DOCUMENT CONTROL DATA - R & D

Security classification of title, body of abstract and indexing annotation must be entered when the overall report is classified

1 ORIGINATING ACTIVITY *(Corporate author)*

Naval Postgraduate School
Monterey, California 93940

2a. REPORT SECURITY CLASSIFICATION

Unclassified

2b. GROUP

3 REPORT TITLE

THE DEFLECTION OF PLANE TURBULENT JETS BY CONVEX WALLS

CORRECTED COPY

4 DESCRIPTIVE NOTES *(Type of report and inclusive dates)*

5 AUTHOR(S) *(First name, middle initial, last name)*

TURGUT SARPKAYA

6 REPORT DATE	7a. TOTAL NO. OF PAGES	7b. NO. OF REFS
27 June 1968	54	23

8a. CONTRACT OR GRANT NO.	9a. ORIGINATOR'S REPORT NUMBER(S)
MIPR No. R-68-4	NPS-59SL8061A
b. PROJECT NO.	
c.	9b. OTHER REPORT NO(S) *(Any other numbers that may be assigned this report)*
d.	

10. DISTRIBUTION STATEMENT

This document has been approved for public release and sale; its distribution is unlimited.

11. SUPPLEMENTARY NOTES	12. SPONSORING MILITARY ACTIVITY
	U. S. Army Materiel Command Harry Diamond Laboratories, Washington, D. C. 20438

13. ABSTRACT

The effects of geometry and Reynolds number on the attachment of a jet to a convex wall and the mechanism of high pressure recovery in convex-walled amplifiers are investigated. The results are presented in terms of normalized parameters in a form suitable for comparison with theoretical results. Reasonably good agreement is obtained between the experimental results and those predicted theoretically by Görtler and Glauert, particularly for regions of flow away from the control port. The effects of the wall setback and control port are most pronounced in a region near the power nozzle where u_m/U_o attains values as high a 1.25.

DD FORM 1 NOV 65 1473 (PAGE 1)

S/N 0101-807-6811

Unclassified

Security Classification

A-31408

14 KEY WORDS	LINK A		LINK B		LINK C	
	ROLE	WT	ROLE	WT	ROLE	WT
Coanda effect Turbulent jet attachment Jet attachment to curved walls Deflection of plane turbulent jets by convex walls						

Sarpkaya
The deflection of plane turbulent jets by convex walls.

4 FEB 69
1 OCT 70
11 Aug'72 INTERLIBRARY LOAN
Motorola, Phoenix, Az.
17768
17338
S10482

QA911
.S2
102887

Sarpkaya
The deflection of plane turbulent jets by convex walls.